C.P. No. 1178

C.P. No. 1178

MINISTRY OF DEFENCE (AVIATION SUPPLY)

AERONAUTICAL RESEARCH COUNCIL

CURRENT PAPERS

Theoretical Pressure Distributions on Four Simple Wing Shapes for a Range of Supersonic Flow Conditions

by

J. Pike

Aerodynamics Dept., R.A.E., Bedford

LONDON: HER MAJESTY'S STATIONERY OFFICE

1971

PRICE *70 p* NET

UDC 533.692.55 : 533.693.3 : 533.6.048.2 : 533.6.011.72 : 533.6.011.5

C.P. No.1178*
March 1971

THEORETICAL PRESSURE DISTRIBUTIONS ON FOUR SIMPLE WING SHAPES FOR A RANGE OF SUPERSONIC FLOW CONDITIONS

by

J. Pike

SUMMARY

Pressure distributions are presented for four conical wing shapes with attached shock waves at their leading edges. The wings are those proposed after Euromech 20 as reference shapes for the comparison of flow prediction methods. The influence on the pressure distribution of wing incidence, free stream Mach number or ratio of specific heats is demonstrated. Some pressure distributions over the upper surface are also presented, assuming an isentropic expansion at the leading edge.

---

* Replaces RAE Technical Report 71064 - ARC 33040

CONTENTS

1 INTRODUCTION

Following Euromech 20 [1] Roe has proposed two caret and two plane delta wings[2] to be used to compare results from various methods for predicting the flow about such wings. In this Report the method of Ref.3 has been used to predict the flow over these wings. This method is only applicable to wings with attached shock waves. It uses a small perturbation technique behind a plane shock wave combined with an empirical modification which tends to reduce the second order errors. The results when compared with known flow conditions[3] show good agreement, except for flows with very large pressure changes in the internal flow. Some comparisons with 'exact' numerical calculations are also shown here (Figs.27-29).

The wing and flow conditions suggested by Roe are shown here in Figs.1-7 reproduced from Ref.2. Fig.1 gives the details of the wings, Fig.2 shows how certain flow regions are labelled. Line PQR represents shock wave detachment, and line SQT the conditions for a plane shock wave. Figs.3-7 show the flow conditions selected and their relation to the regions of Fig.2. The numbers form part of a general labelling system, used to label Figs.8-39, of the form:-

letter A to D denoting the wing as in Fig.1;

digit 0-9 denoting Mach number according to the code 0 for 2.6, 1 for 3, 2 for 3.5, 3 for 4, 4 for 4.5, 5 for 5, 6 for 6, 7 for 7.5, 8 for 8, 9 for 10;

digit 1-5 in order of ascending angle of incidence;

letter U or L denoting the flow over the upper or lower surfaces, respectively;

below this label, the values of the flow variables γ, M and α are indicated, as also is the flow regime (A, B, C or D) according to the classification of Fig.2.

For example, the plot in Fig.27 is labelled D31L, with 1.4, 4, 5, B below. This denotes the lower surface of the delta wing with the leading edge having a sweep angle of 50° at flow condition 31 (see Fig.7). Flow condition 31 means $M_{\infty} = 4$ and $\alpha = 5$, as is shown in Fig.7. Also included in the table is the information that $\gamma = 1.4$ and the flow regime is of type B (see Fig.2).

2 THE PRESSURE DISTRIBUTIONS

Near the lines PU and SQ of Fig.2, the pressure distribution can be obtained[3] by linearising about either the free stream or the parallel flow behind a plane shock wave. A simple semi-empirical formula has been developed[3] which includes both of these cases in a single expression. This expression has been shown to give good estimates of the pressure distributions over the whole of regions A and B except near the boundary line PQT. It has also been applied to the upper surfaces, although it is only theoretically justifiable for small upper surface incidence.

Figs.8-10 each show the pressure distribution for a wing over a range of incidence at the same Mach number. Fig.8 shows wing A at M = 10. Fig.9 shows wing B for M = 5, Fig.10 shows wing D at M = 4. Both upper and lower surface pressure distributions are shown for γ = 1.4 and 1.25. It can be observed that changing γ makes very little difference to the pressure distribution at low incidence, but near detachment significant changes occur both in the pressure coefficients and the detachment conditions.

The results of a systematic investigation of all the conditions proposed by Roe are summarised in Tables 1-4 for wings A to D. Wing A has finite thickness, and for conditions 1, 12, 21, 42, 62 and 92 the upper surface is very nearly streamwise. For region D, all the leading edge shock waves were found to be detached including that of B33 (see Figs.4 and 5). The wing and flow conditions where the leading edge is subsonic are listed in Tables 1-4. For the conditions A41, the upper surface shock wave is detached, causing an otherwise attached lower surface shock wave to be detached also. It should be noted that the lower surface pressure distribution of Fig.11 does not allow for upper surface influence.

The lower surface pressure distributions for regions A and B are shown in Figs.11-29 with y/y_{max} a spanwise coordinate normal to the ridge line. The C_p axis has a false zero to accentuate the pressure changes. The ratio of the C_p scale to the y/y_{max} scale is given by the value of r, shown near the C_p axis. Each pressure distribution has been given a separate figure to facilitate the comparison with other estimates. Only limited comment is included here on the pressure distributions, a critical assessment being left until after the comparisons have been made.

The region of constant pressure coefficient near the leading edge is obtained from oblique shock wave theory[4], and is exact over the conically

supersonic region of the wing for inviscid flow. For the flow conditions of region B, where an expansion occurs near the centre of the wing, the true position of the conical sonic point is indicated. For region A, the pressure rise shown may indicate the presence of a second shock wave and the conically sonic position can no longer be obtained from the exact leading-edge conditions. Near detachment in region B, the present theory predicts too large a region of constant pressure, as shown particularly in Fig.26. For most of regions A and B, away from the boundary line PQT the pressure distributions have been found to be surprisingly accurate[3]. Comparison with the results of Voskresenskii[5] for plane deltas is shown in Figs.27–29. Unfortunately it is difficult to plot the results (taken from Ref.6) accurately on the expanded scale used. However the best estimate of them corresponds closely with the predicted pressures, except for the region of rapid pressure change in D33.

Figs.30–39 show a selection of upper surface pressure distributions, which tend to indicate that the variation in the pressure on the upper surface is much smaller than on the lower surfaces.

In Figs.8–39 the average pressure coefficient $(\bar{C}_p)$ is indicated. The lift coefficient of the wing is of course the difference between $\bar{C}_p$ on the upper surface, and $\bar{C}_p$ on the lower surface. Also shown is the pressure coefficient on an unswept wedge at the same incidence and Mach number (C_{pw}).

The time to evaluate a pressure distribution using an ICL 4130 computer was about ½ second to find C_{pe} and C_{pw}, plus 1/20 second for each pressure value.

Table 1

WING A, $\gamma = 1.4$

A1	Subsonic leading edge
A11	Shock wave detached
A12	Subsonic leading edge
A21	Shock wave detached
A41	Fig.11 NB. Upper surface shock wave detached
A42	Shock wave detached
A43	Shock wave detached
A61	Fig.12
A62	Fig.13
A63	Shock wave detached
A81	Fig.14
A82	Fig.15
A83	Shock wave detached
A91	Figs.8, 16 and 30
A92	Figs.8 and 17
A93	Figs.8, 18 and 31
A94	Figs.8 and 19
A95	Shock wave detached

Table 2

WING B, $\gamma = 1.4$

B11	Shock wave detached
B12	Shock wave detached
B13	Shock wave detached
B31	Fig.20
B32	Fig.21
B33	Shock wave detached
B34	Shock wave detached
B51	Figs.9, 22 and 32
B52	Figs.9, 23 and 33
B53	Thin wing leading edge subsonic
B54	Thin wing leading edge subsonic
B55	Shock wave detached
B71	Figs.24 and 34
B72	Thin wing leading edge subsonic
B73	Thin wing leading edge subsonic
B74	Equivalent wedge shock wave detached

Table 3

WING C, $\gamma = 1.4$

C11	Subsonic leading edge
C12	Subsonic leading edge
C13	Shock wave detached
C41	Shock wave detached
C42	Shock wave detached
C43	Shock wave detached
C91	Figs.25 and 35
C92	Figs.26 and 36
C93	Shock wave detached
C94	Shock wave detached

Table 4

WING D, $\gamma = 1.4$

D31	Figs.10, 27 and 37
D32	Figs.10, 28 and 38
D33	Figs.10, 29 and 39

REFERENCES

No.	Author(s)	Title, etc.
1	P.L. Roe L. Davies L.C. Squire	Report on Euromech 20. RAE Technical Report 71054 (1971)
2	P.L. Roe	Unpublished RAE Memorandum
3	J. Pike	The flow past flat and anhedral delta wings with attached shock waves. Unpublished RAE Report
4	J. Pike	Attached flow conditions on sharp supersonic leading edges. Unpublished RAE Report
5	G.P. Voskresenskii	Numerical solution of the problem of a supersonic gas flow past an arbitrary surface of a delta wing in the compression region. Izv. Akad. Nauk. SSSR, Mekh. Zhid. 1. Gaza, 4 (1968)
6	J.C. South, Jnr. E.B. Klunker	Methods for calculating non-linear conical flows. NASA SP 228 (1969)

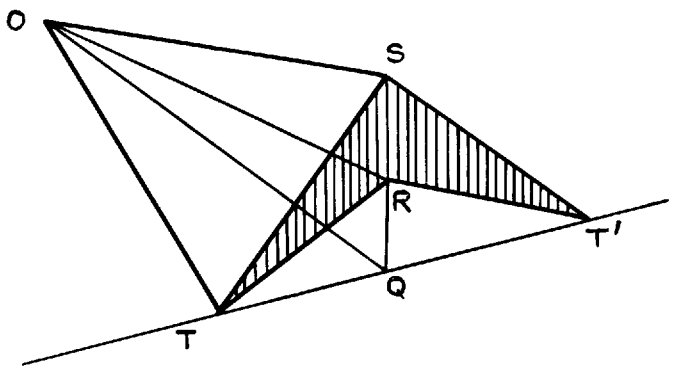

	QOR	ROS	OTQ	TRT'
A	6·51	7·49	73·77	137·44
B	12·00	0	75·00	104·38
C	0	0	75·00	180·00
D	0	0	50·00	180·00

Notes

1 Wing A has a 'releastic' thickness. The others are assumed ideally thin

2 The values quoted for angle TRT' is the true angle between the facets ORT, ORT' , ie it is measured normal to the line OR

Fig.1 Angles defining the standard wings

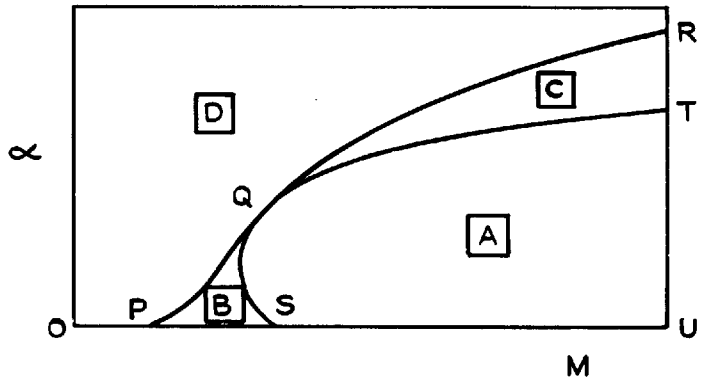

α is the incidence of the line OR

Fig.2 Schematic $(M\alpha)$ diagram

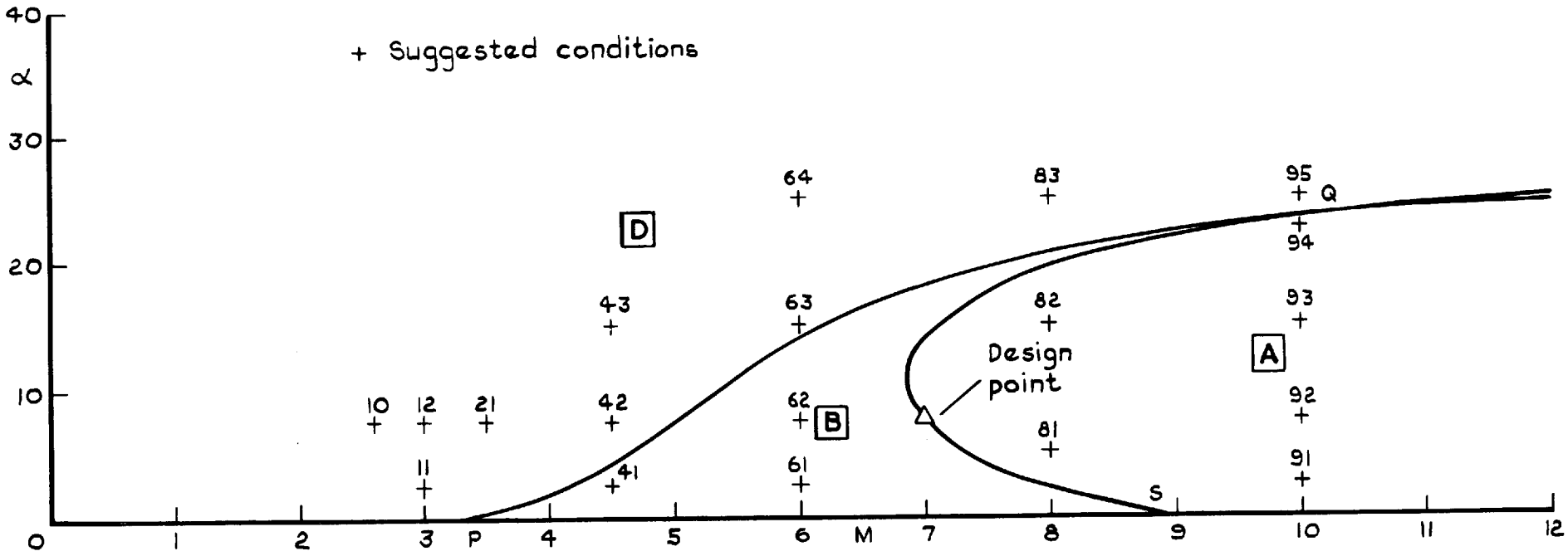
+ Suggested conditions
α
40
30
20
10
0
1
2
3
P
4
5
6
M
7
8
9
10
11
12
D
B
A
Design point
S
Q
10
12
21
11
42
41
43
62
61
63
64
82
81
83
92
91
93
94
95

Fig.3 Wing A

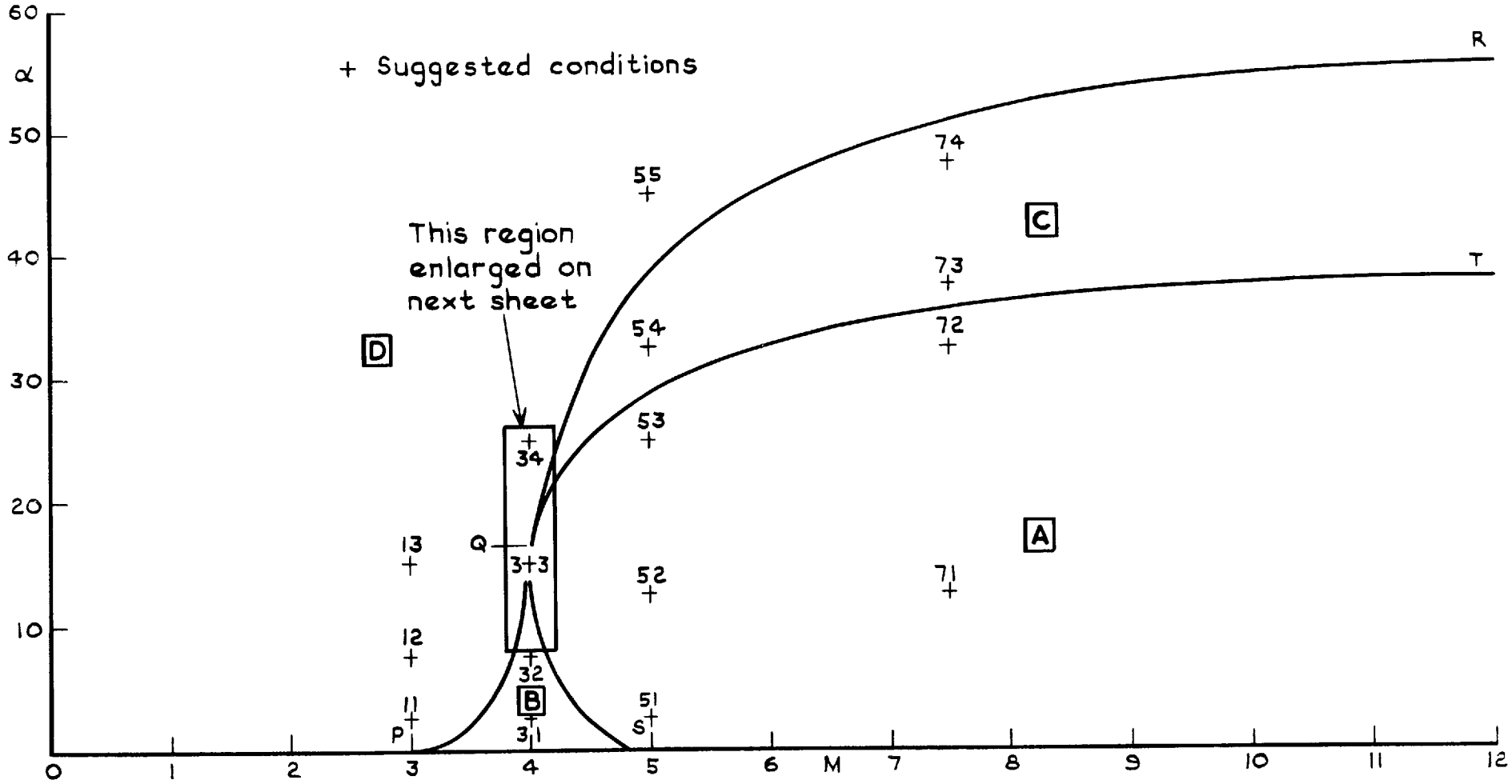
+ Suggested conditions
This region enlarged on next sheet
α
60
50
40
30
20
10
0
1
2
3
4
5
6
M
7
8
9
10
11
12
R
T
A
B
C
D
Q
P
S
74
55
73
54
72
53
34
13
3+3
52
71
12
32
11
51
31

Fig. 4 Wing B

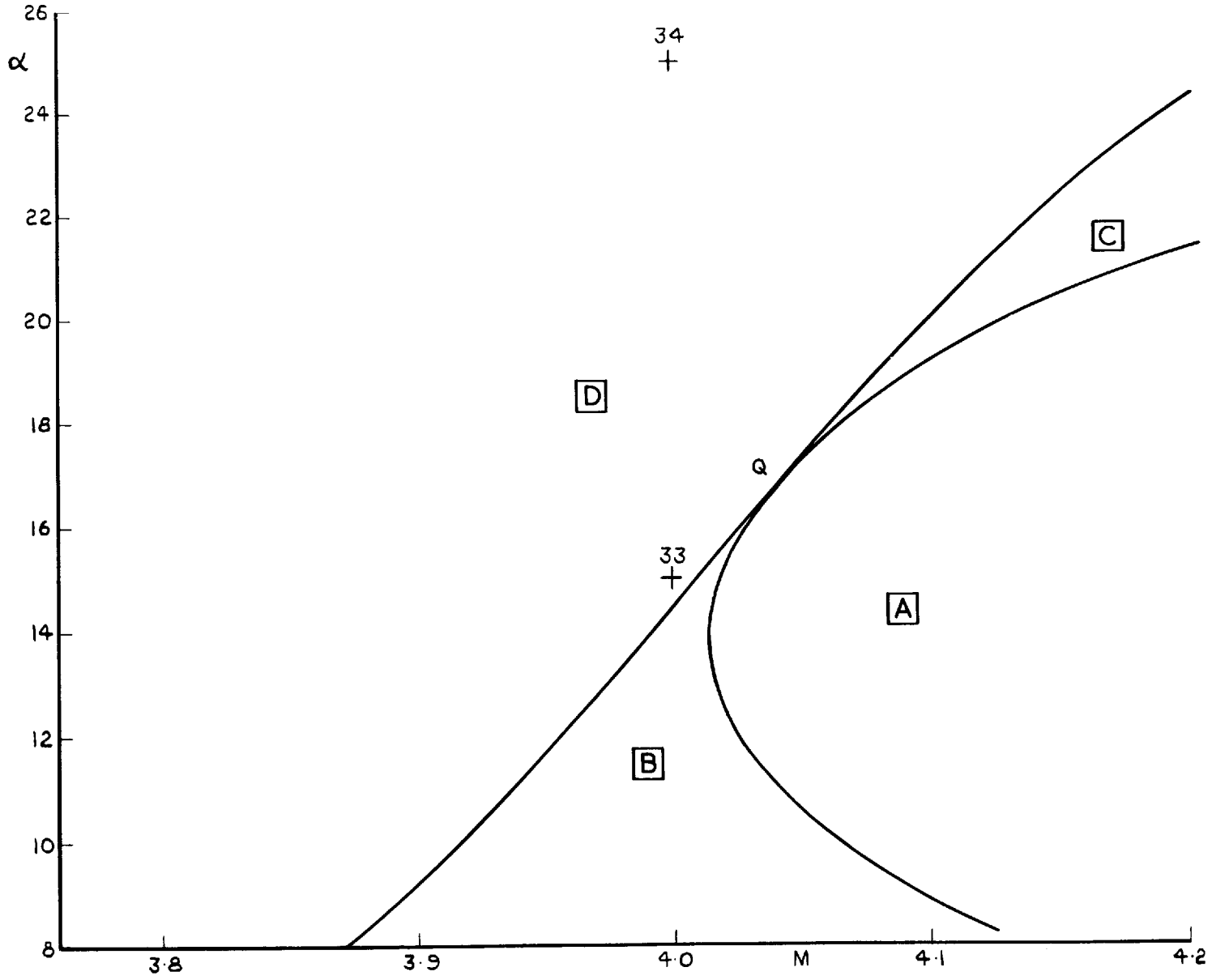

Fig.5 Wing B (enlargement)

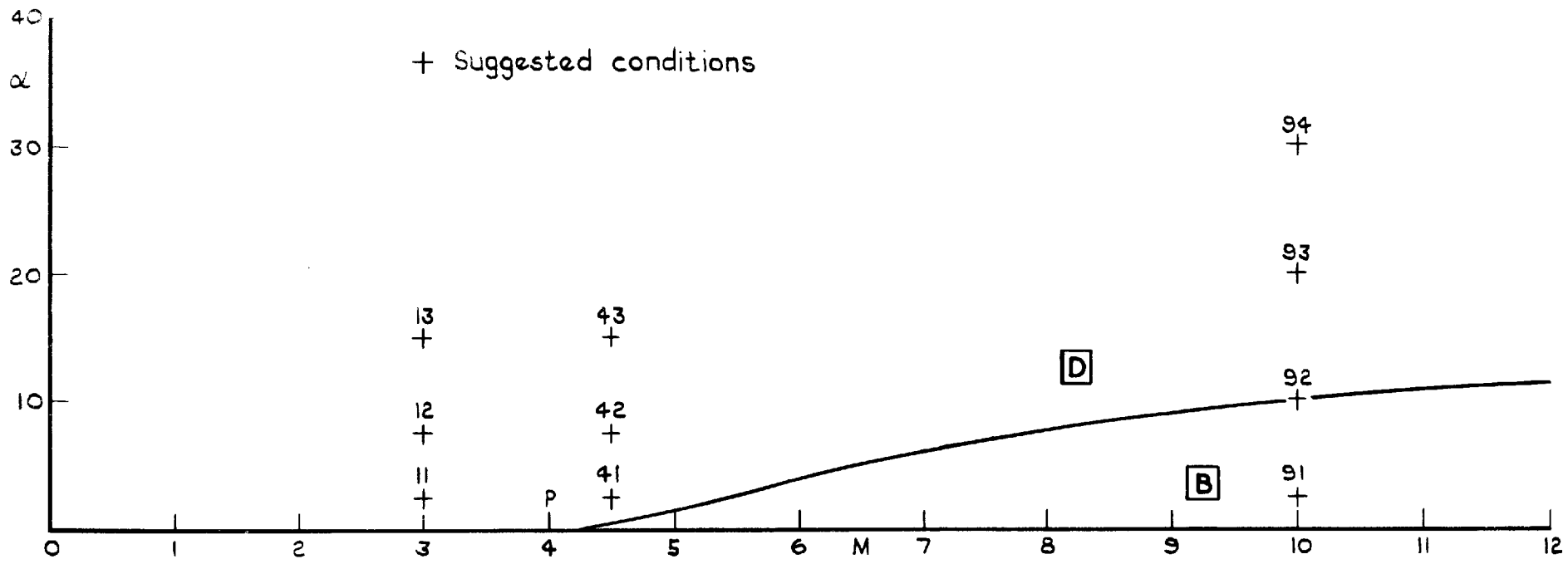
40
α
30
20
10
+ Suggested conditions
13
43
12
42
11
41
P
94
93
92
91
D
B
0
1
2
3
4
5
6
M
7
8
9
10
11
12

Fig.6 Wing C

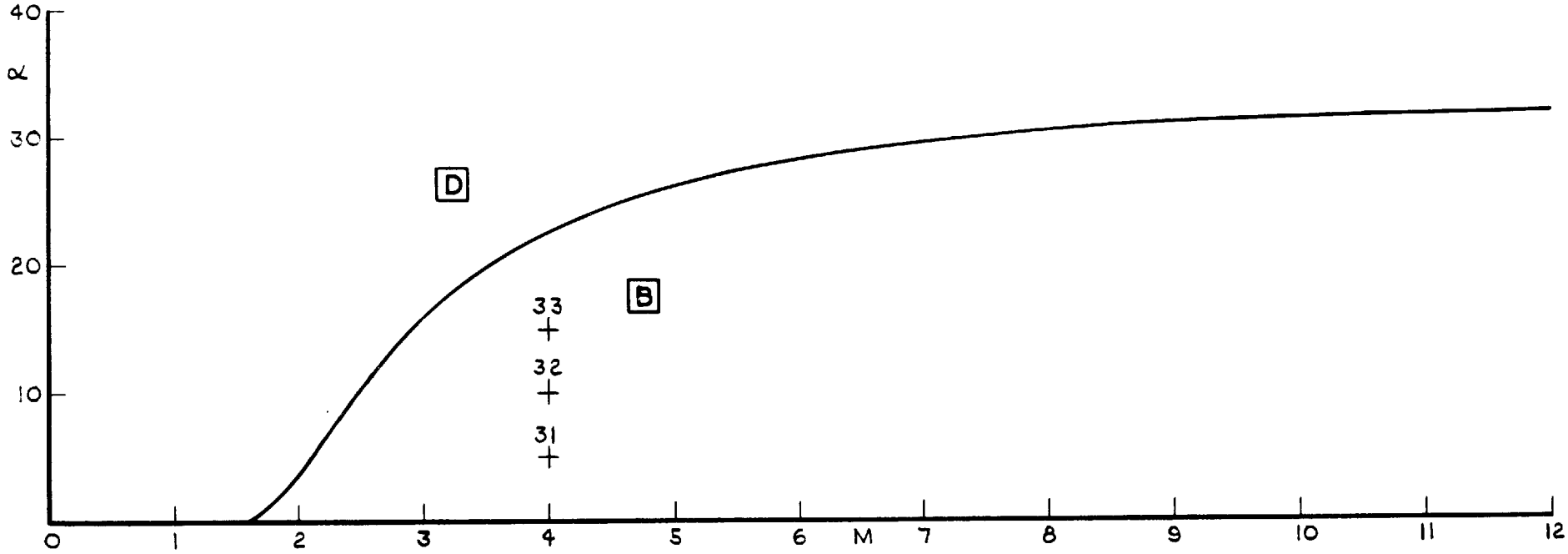

Fig. 7 Wing D

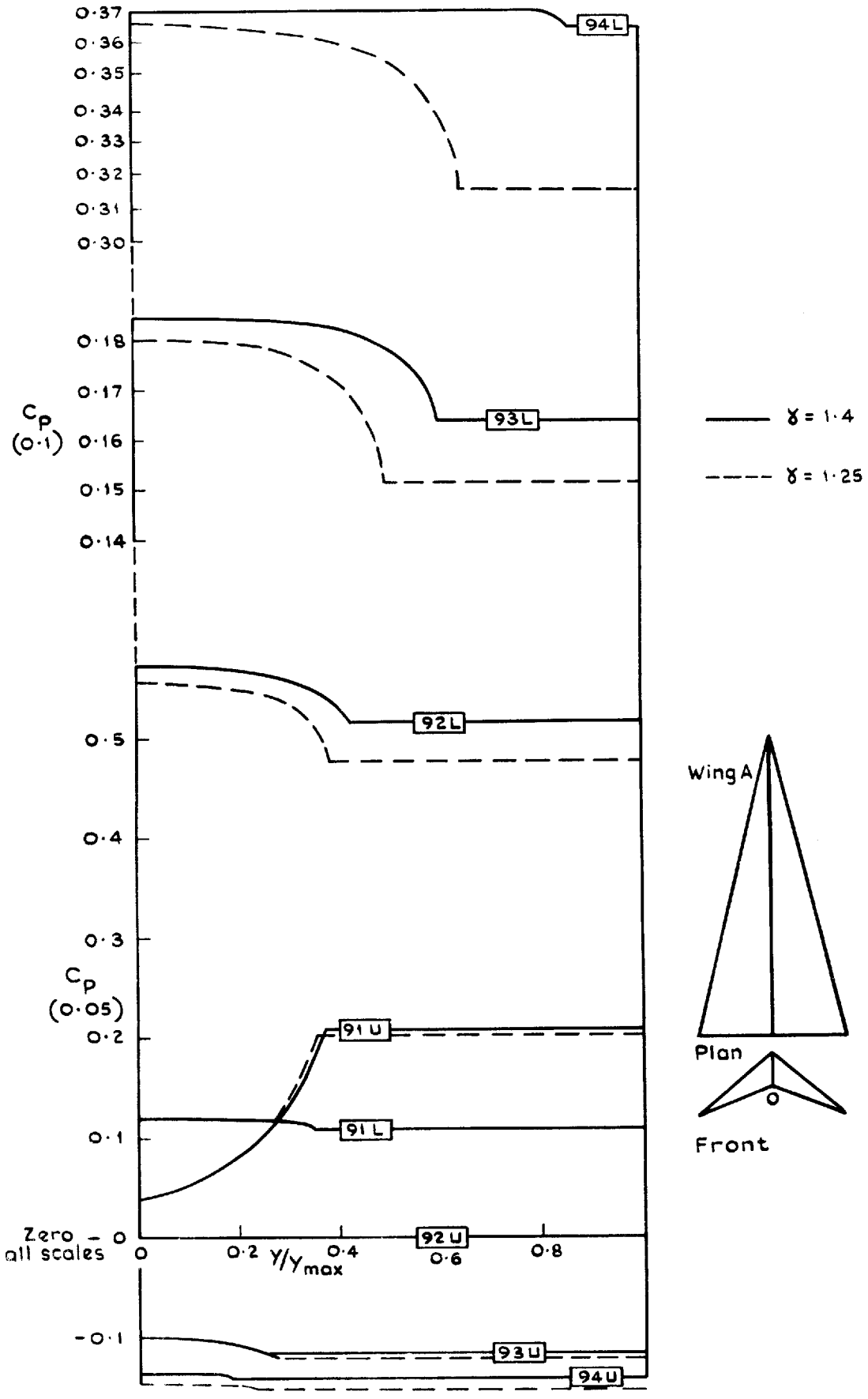

Fig.8 Wing A: Surface pressure coefficients on the upper and lower surfaces at M=10

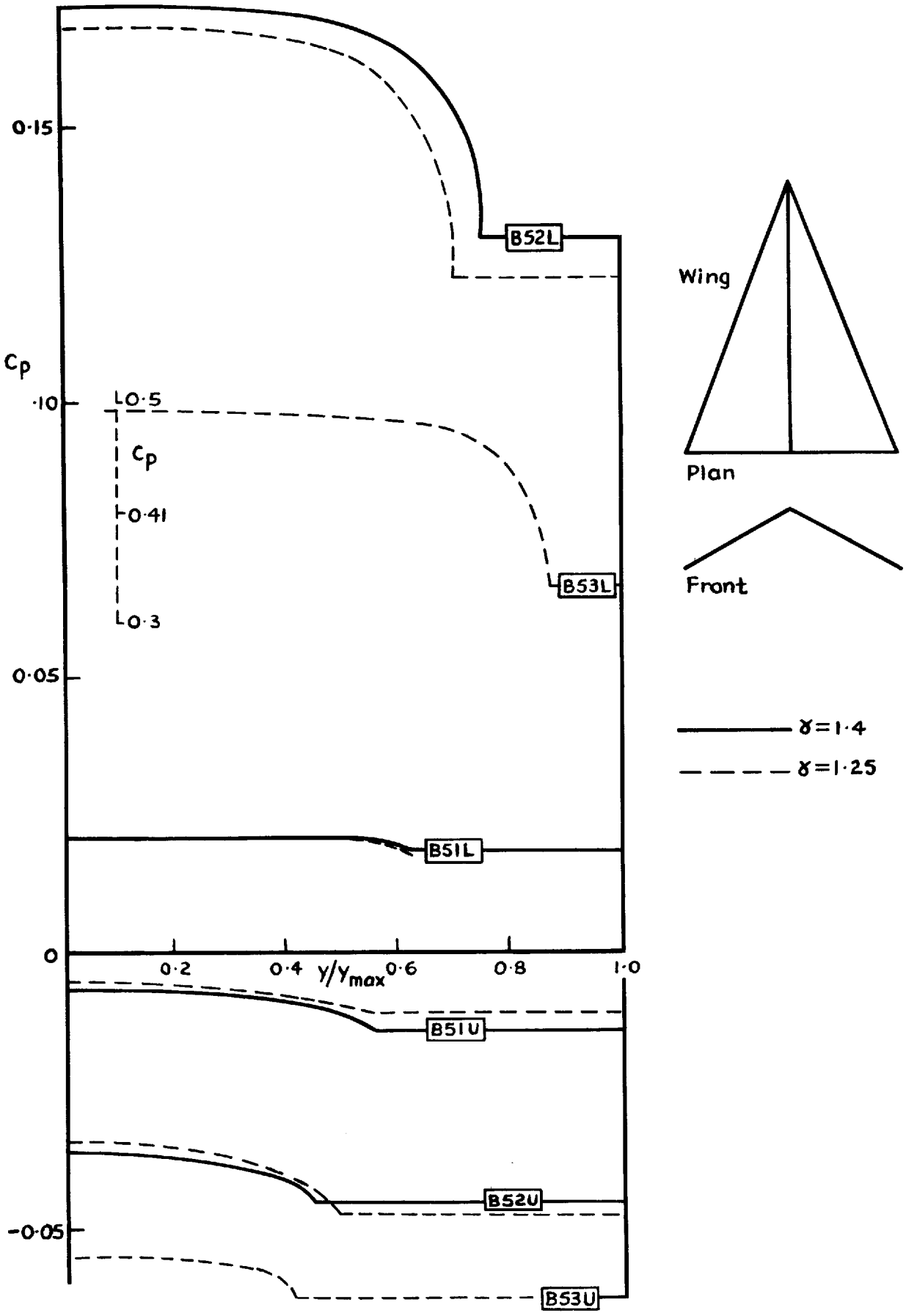

Fig.9 Wing B: Surface pressure coefficient on the upper and lower surfaces at M=5

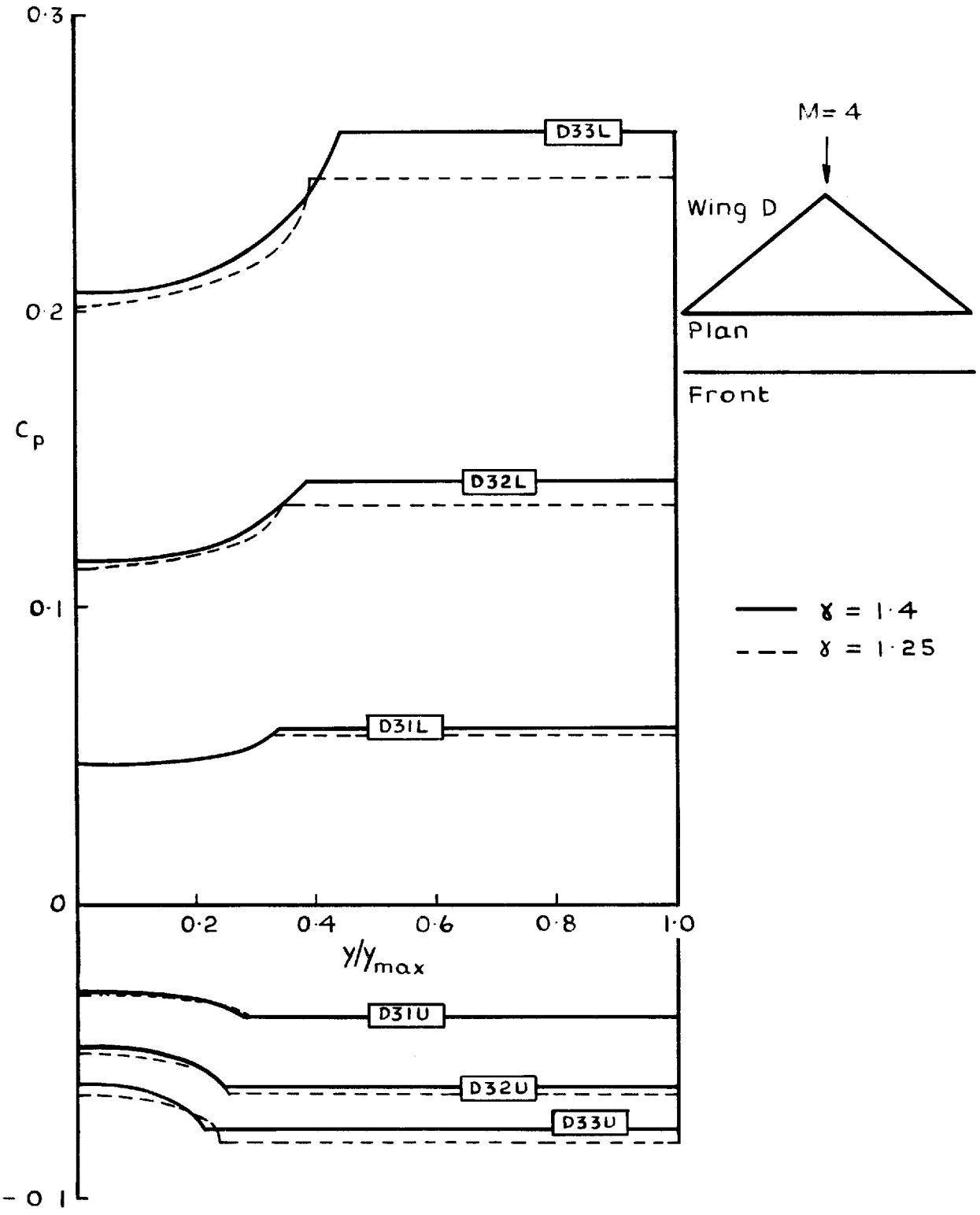

Fig.10 Wing D: Surface pressure coefficient on the upper and lower surfaces at M = 4

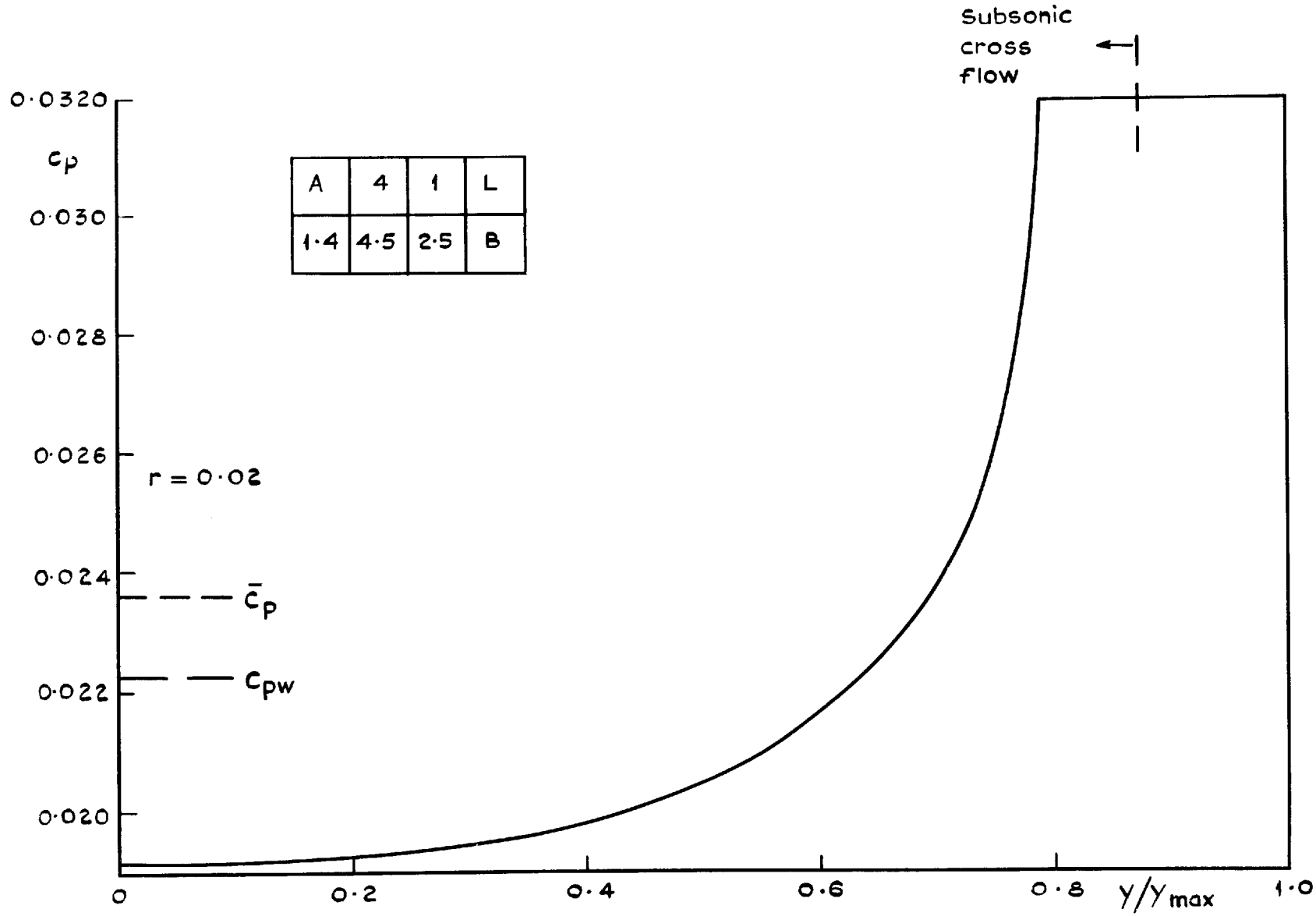

Fig. 11 Wing A : Pressure distribution across span $M = 4 \cdot 5$, $\gamma = 1 \cdot 4$, $\alpha = 2 \cdot 5^\circ$

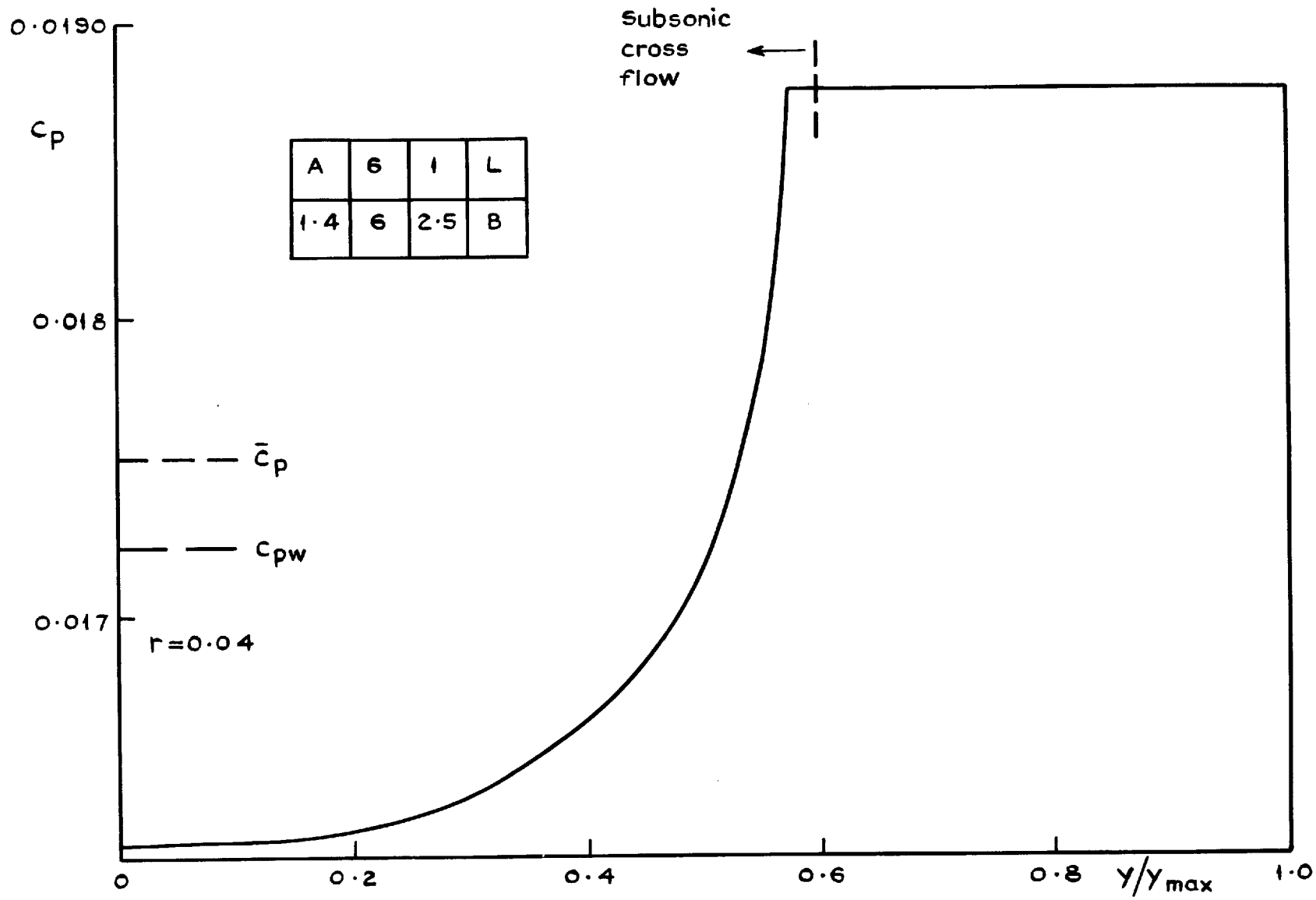

Fig. 12 Wing A: Pressure distribution across span $M=6$, $\gamma=1\cdot4$, $\alpha=2\cdot5$

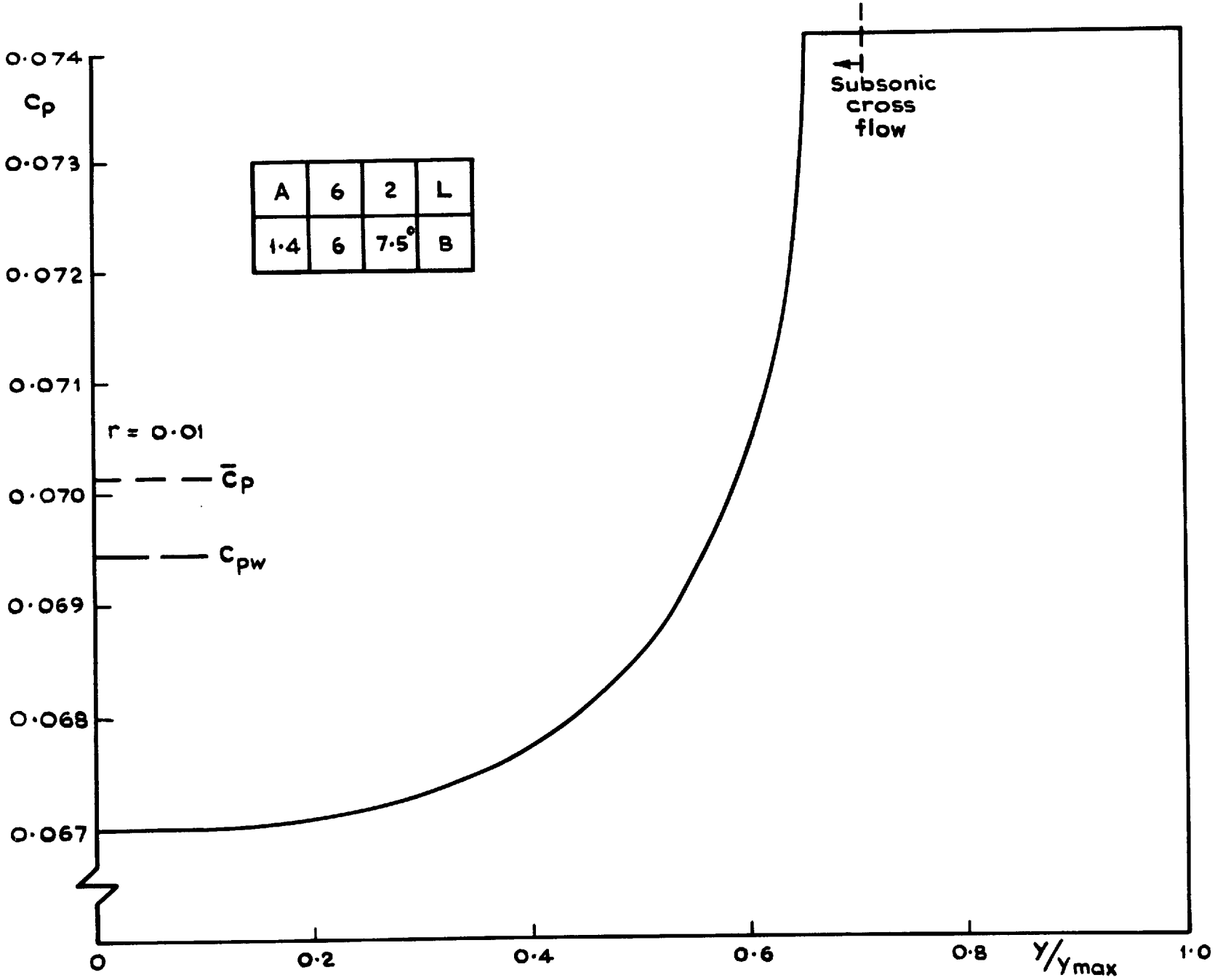

Fig. 13 Wing A: Pressure distribution across span $M = 6$, $\gamma = 1{\cdot}4$, $\alpha = 7{\cdot}5^\circ$

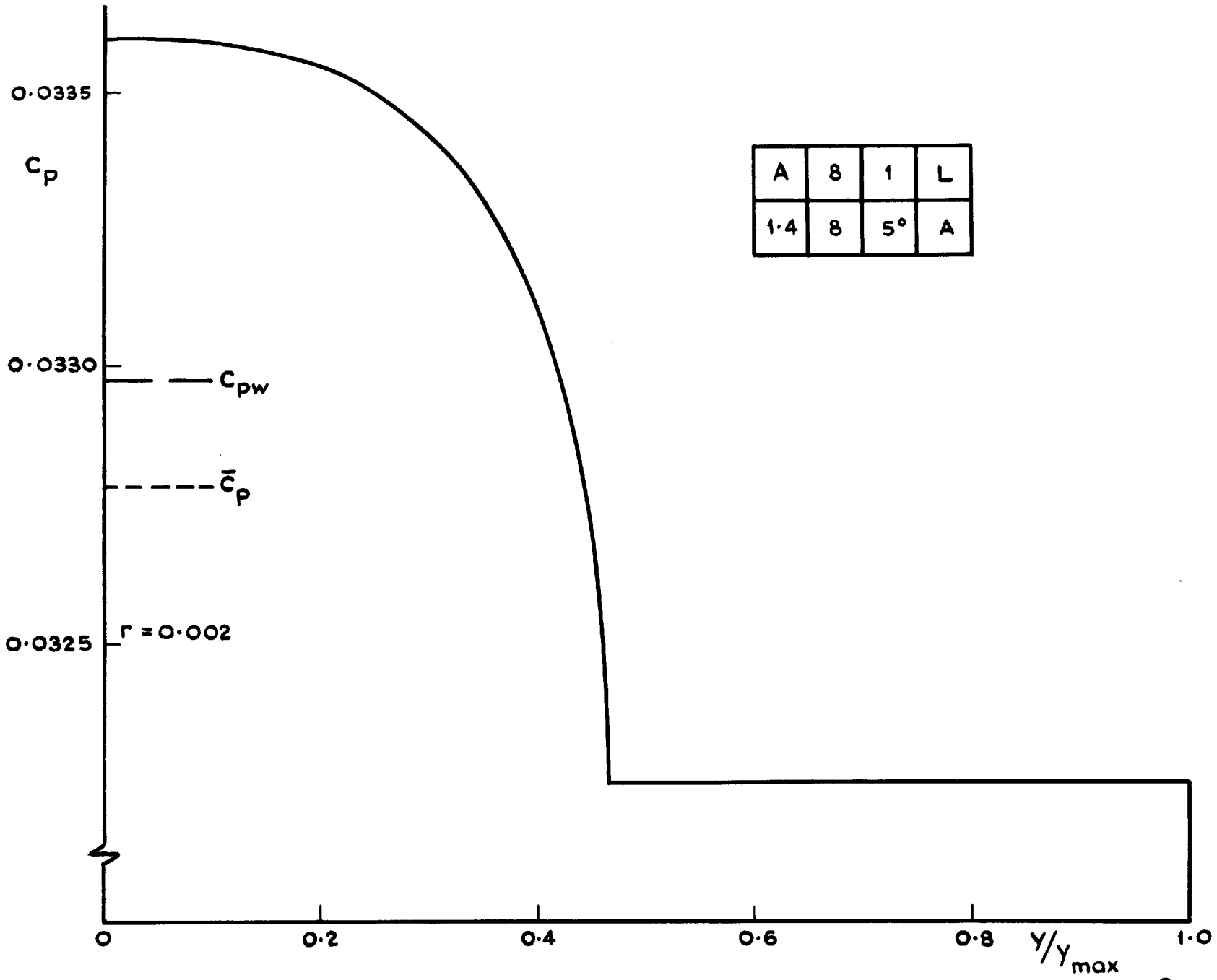

Fig.14 Wing A: Pressure distribution across span $M=8$, $\gamma=1\cdot4$, $\alpha=5^\circ$

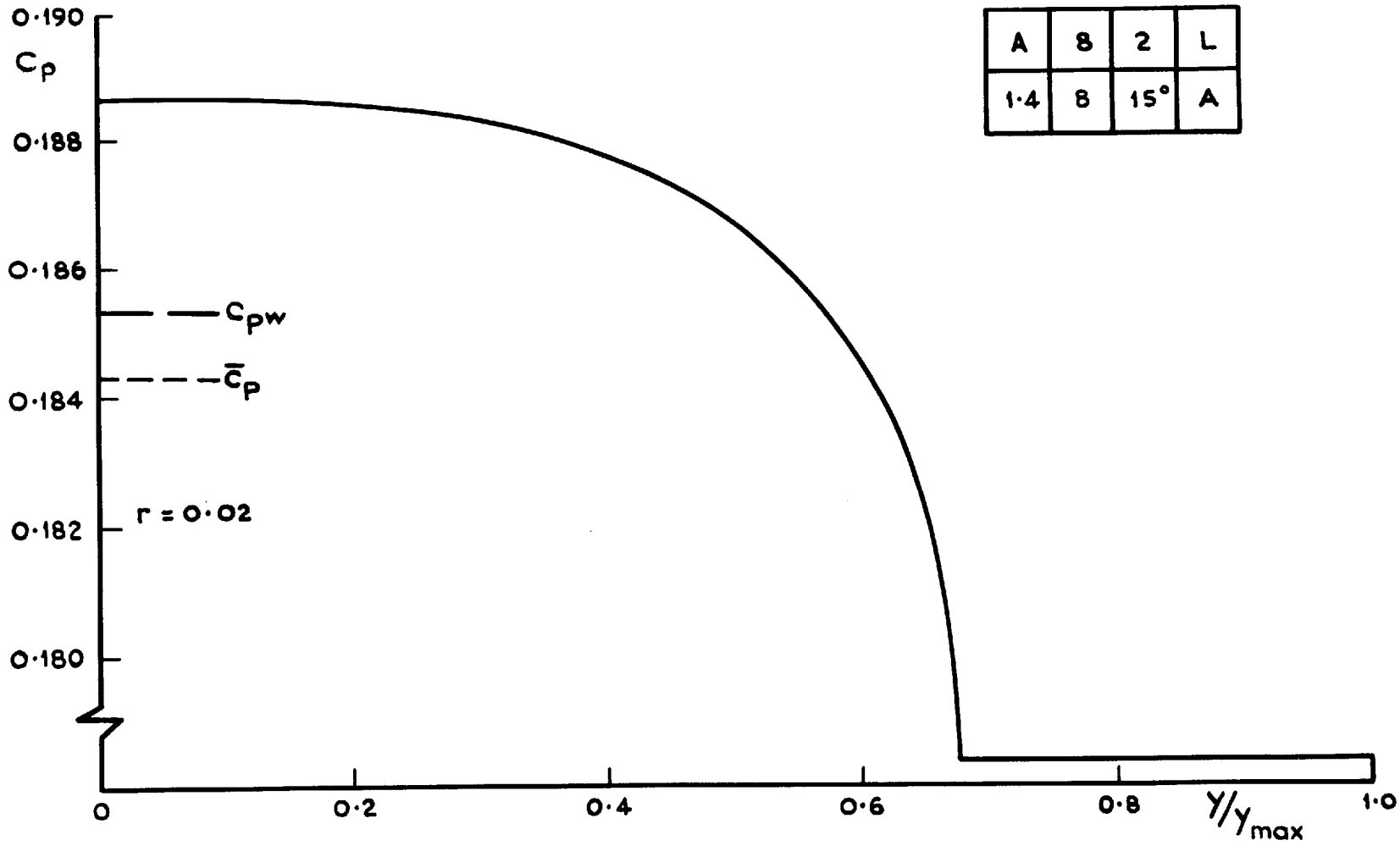

Fig. 15 Wing A: Pressure distribution across span $M = 8$, $\gamma = 1{\cdot}4$, $\alpha = 15^\circ$

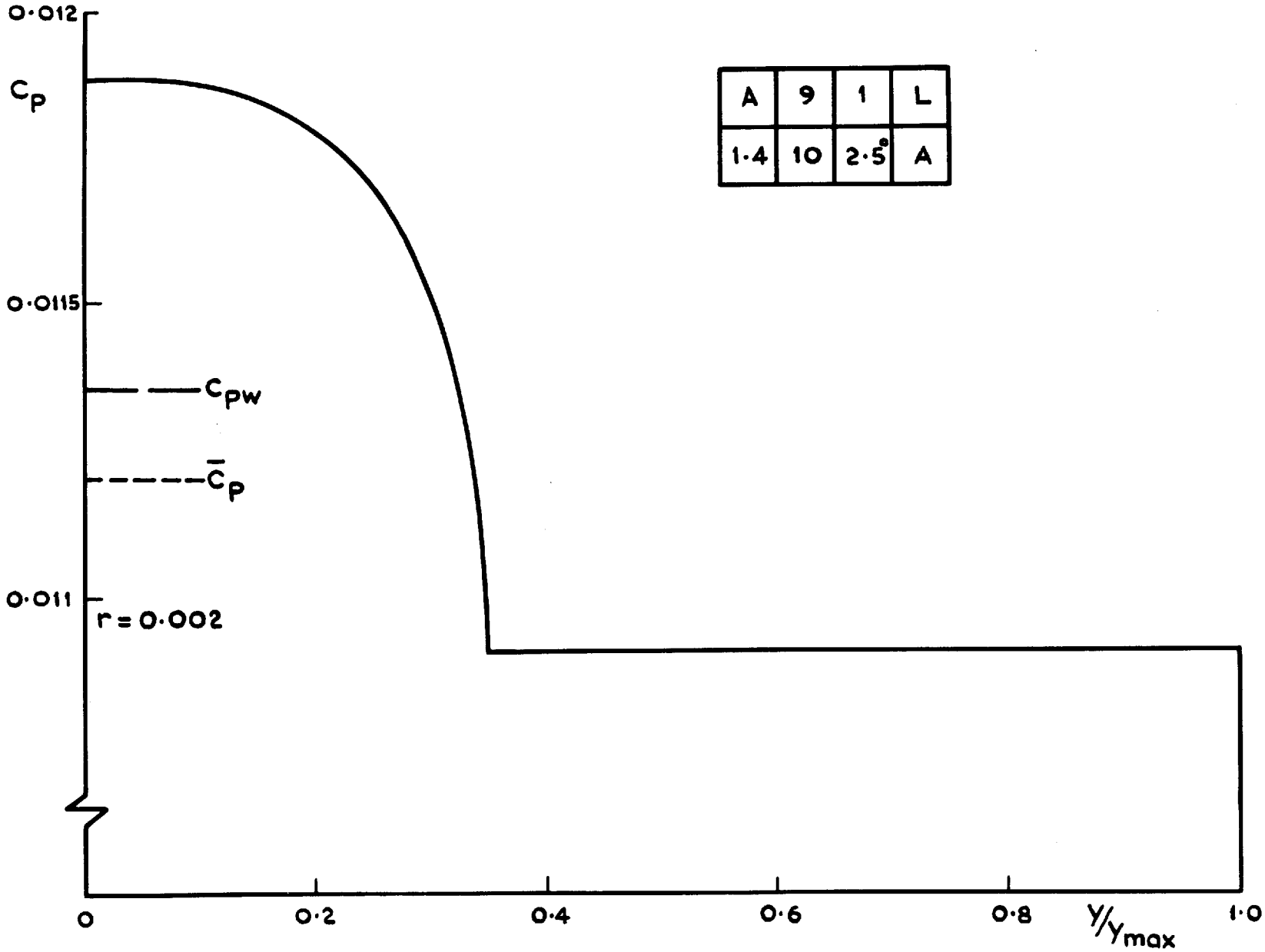

Fig. 16 Wing A: Pressure distribution lower surface $M = 10$, $\gamma = 1{\cdot}4$, $\alpha = 2{\cdot}5^\circ$

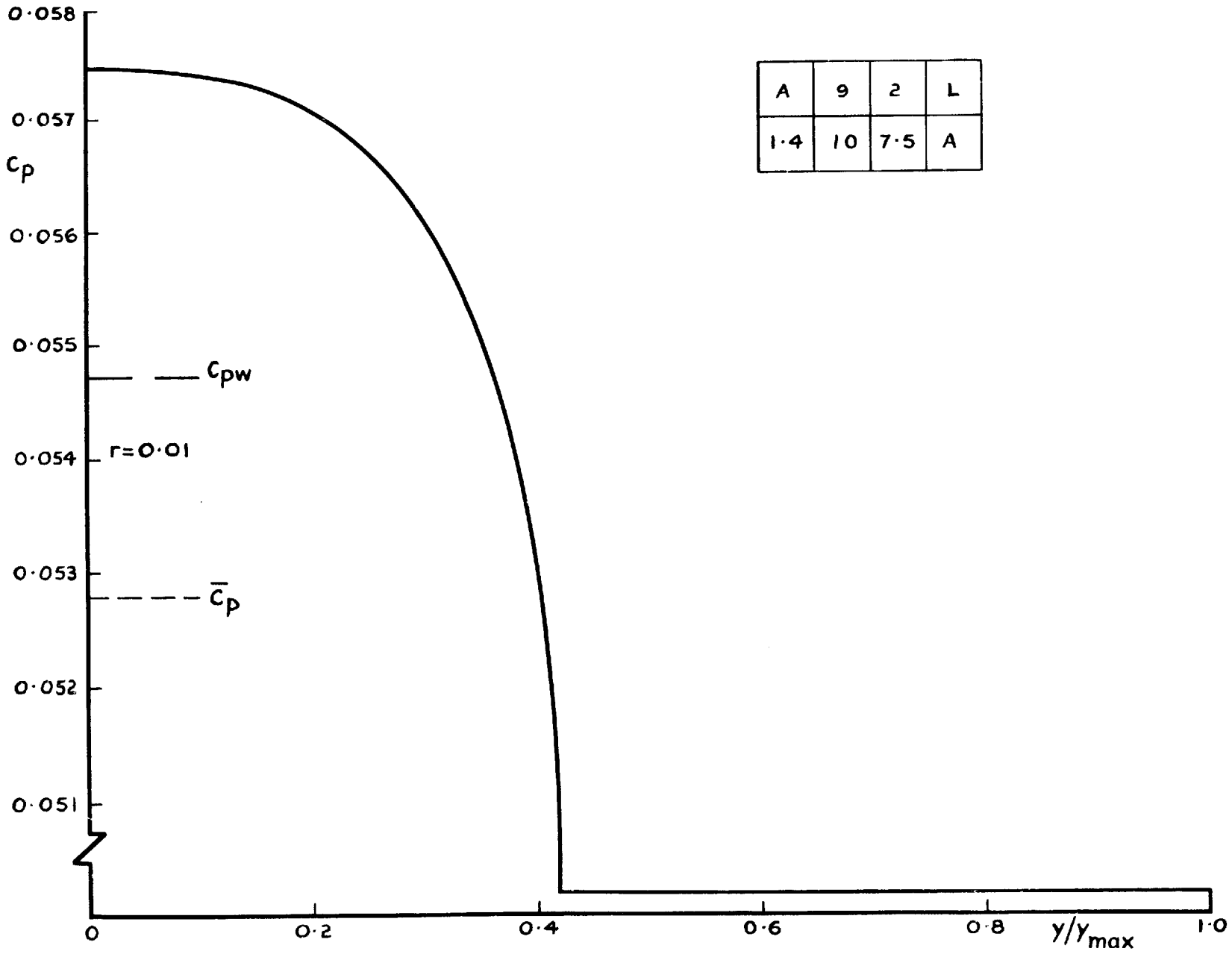

Fig.17 Wing A: Pressure distribution upper surface M=10, γ=1·4, α = 7·5

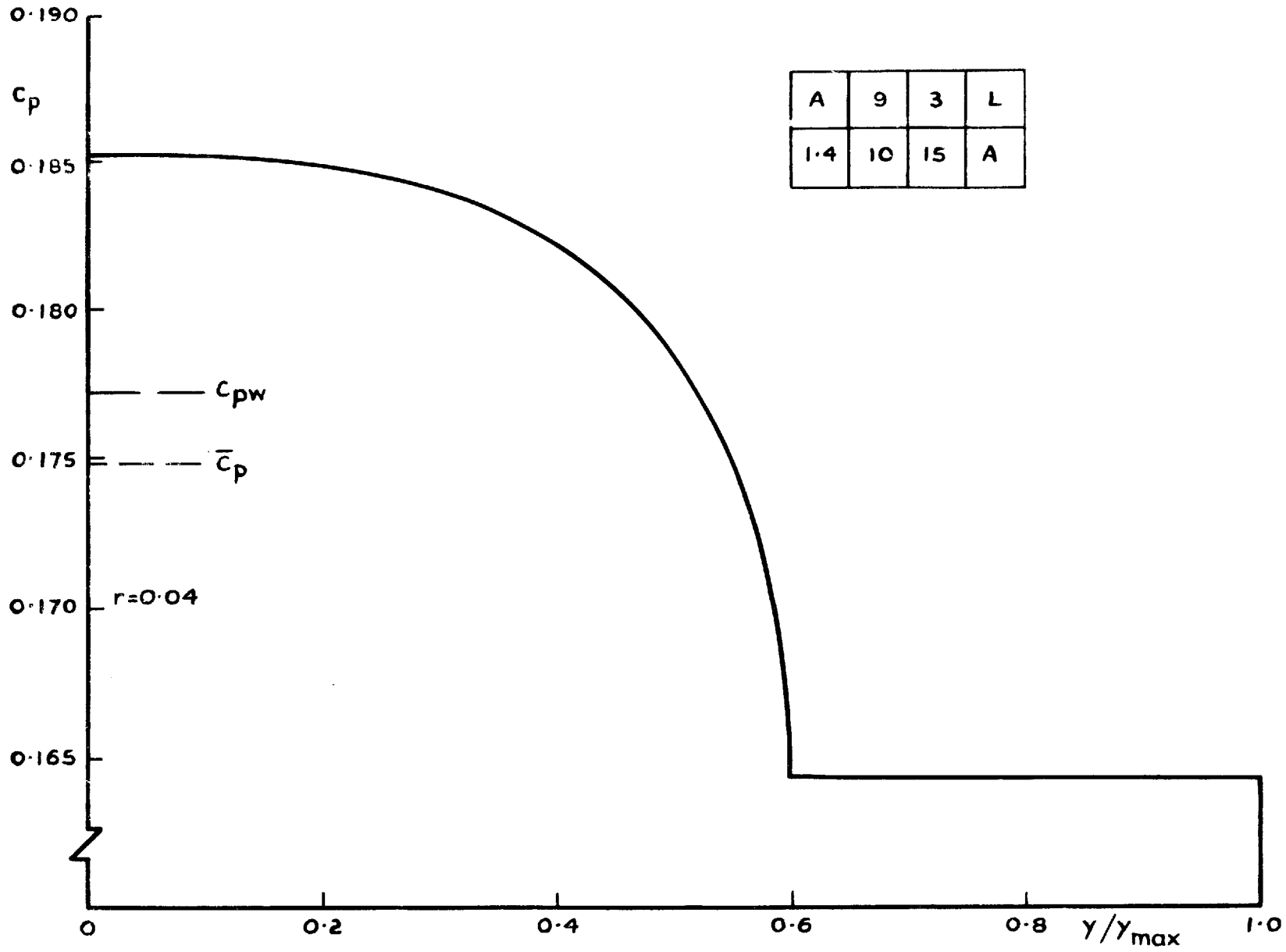

Fig.18 Wing A: Pressure distribution lower surface M=10, γ=1·4, $\alpha = 15^{\circ}$

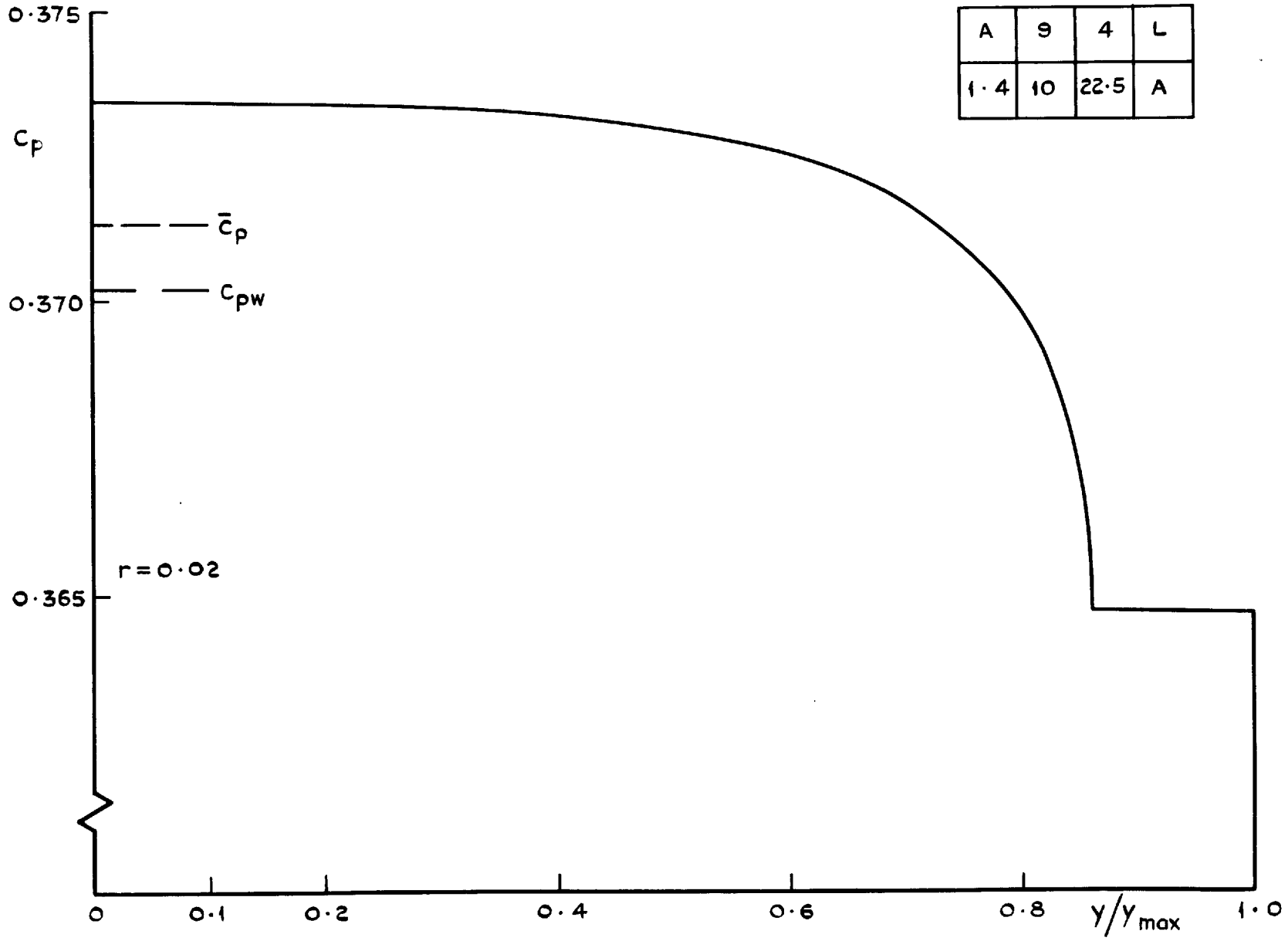

Fig.19 Wing A : Pressure distribution upper surface $M=10$, $\gamma=1\cdot4$, $\alpha=22\cdot5$

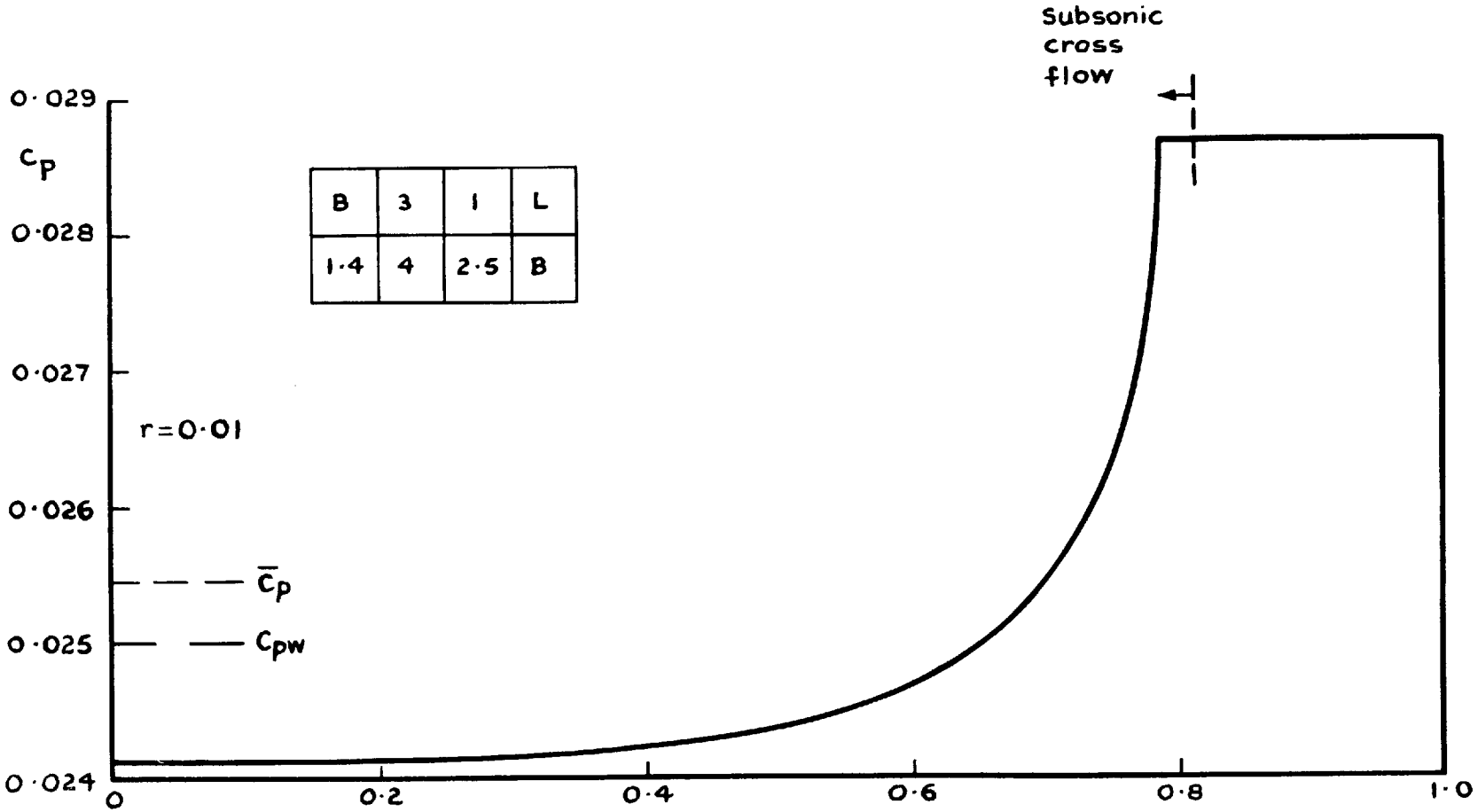

Fig.20 Wing B: Pressure distribution lower surface M=4, γ=1·4, α=2·5°

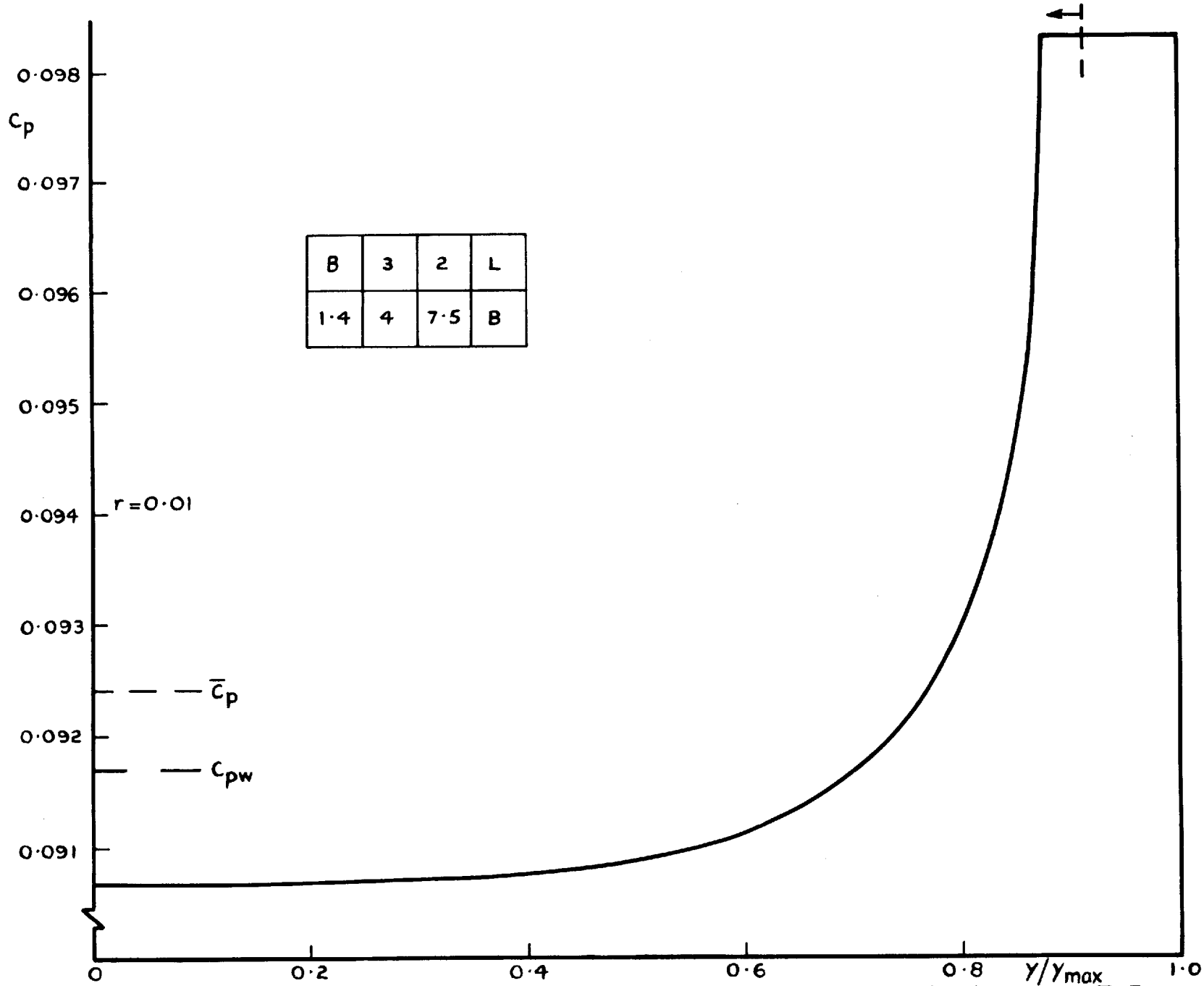

Fig.21 Wing B: Pressure distribution lower surface $M=4$, $\gamma=1{\cdot}4$, $\alpha=7{\cdot}5$

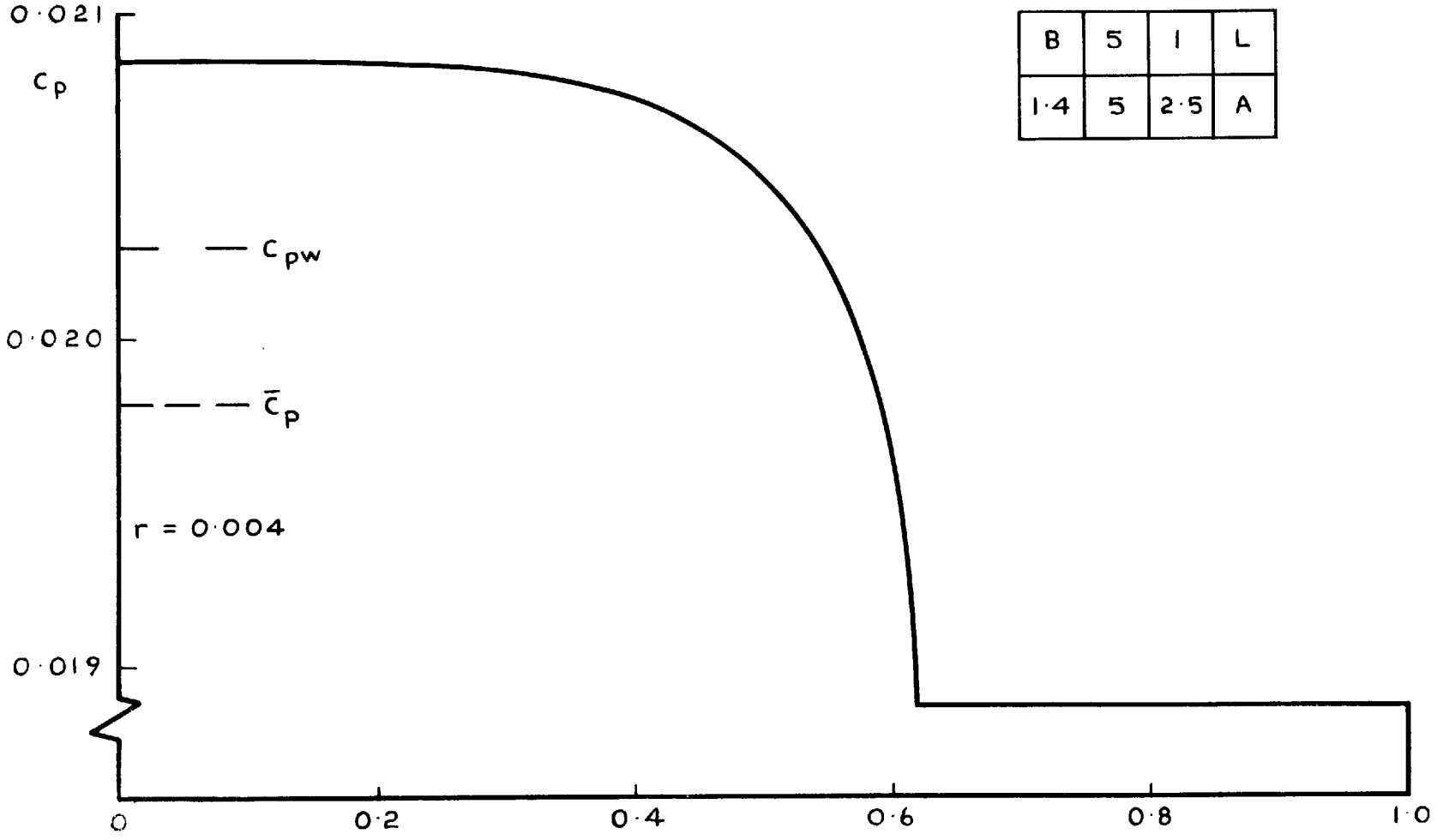

Fig. 22 Wing B: Pressure distribution lower surface M = 5, γ = 1·4, α = 2·5°

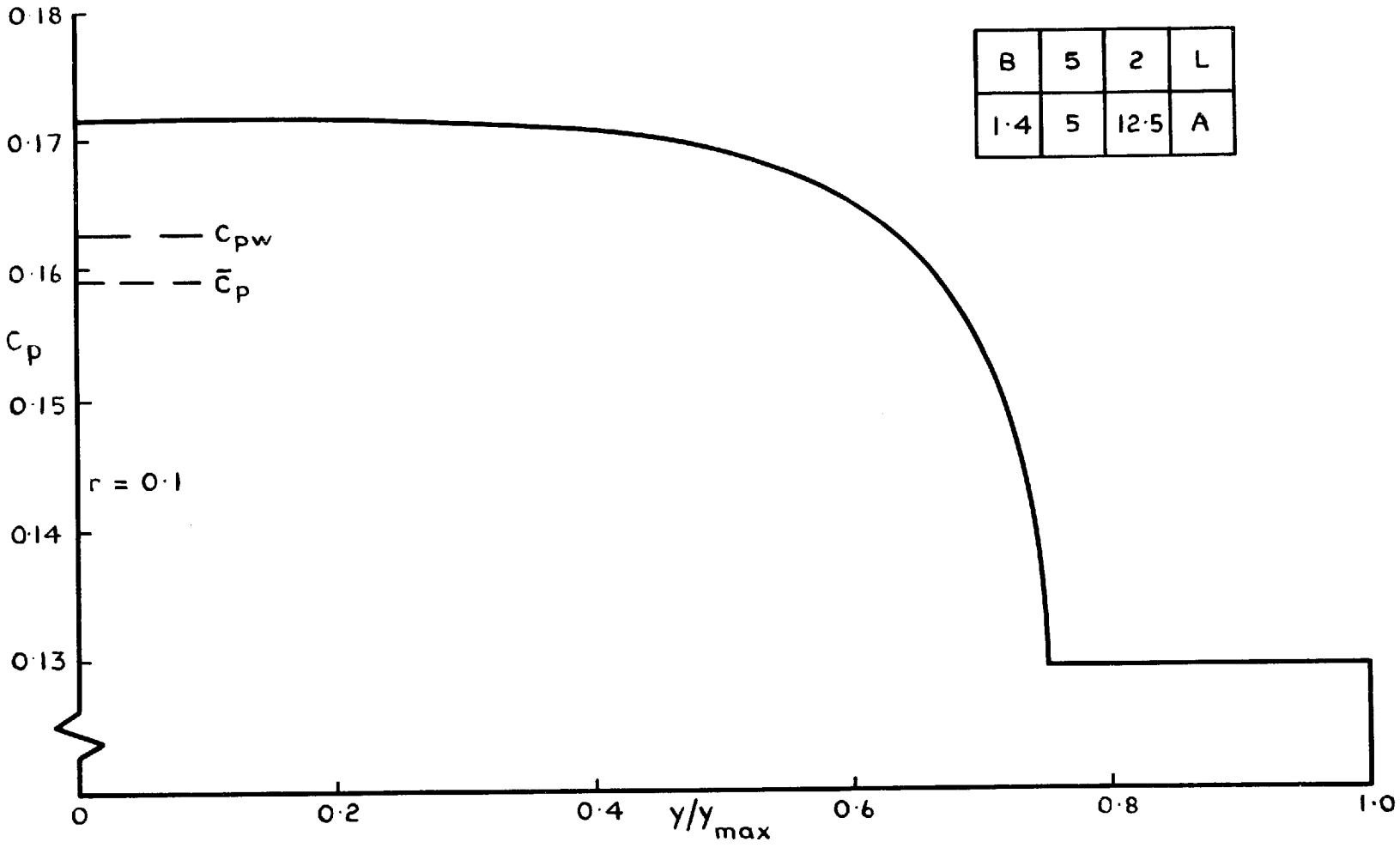

Fig. 23 Wing B: Pressure distribution lower surface $M = 5$, $\gamma = 1{\cdot}4$, $\alpha = 12{\cdot}5^{\circ}$

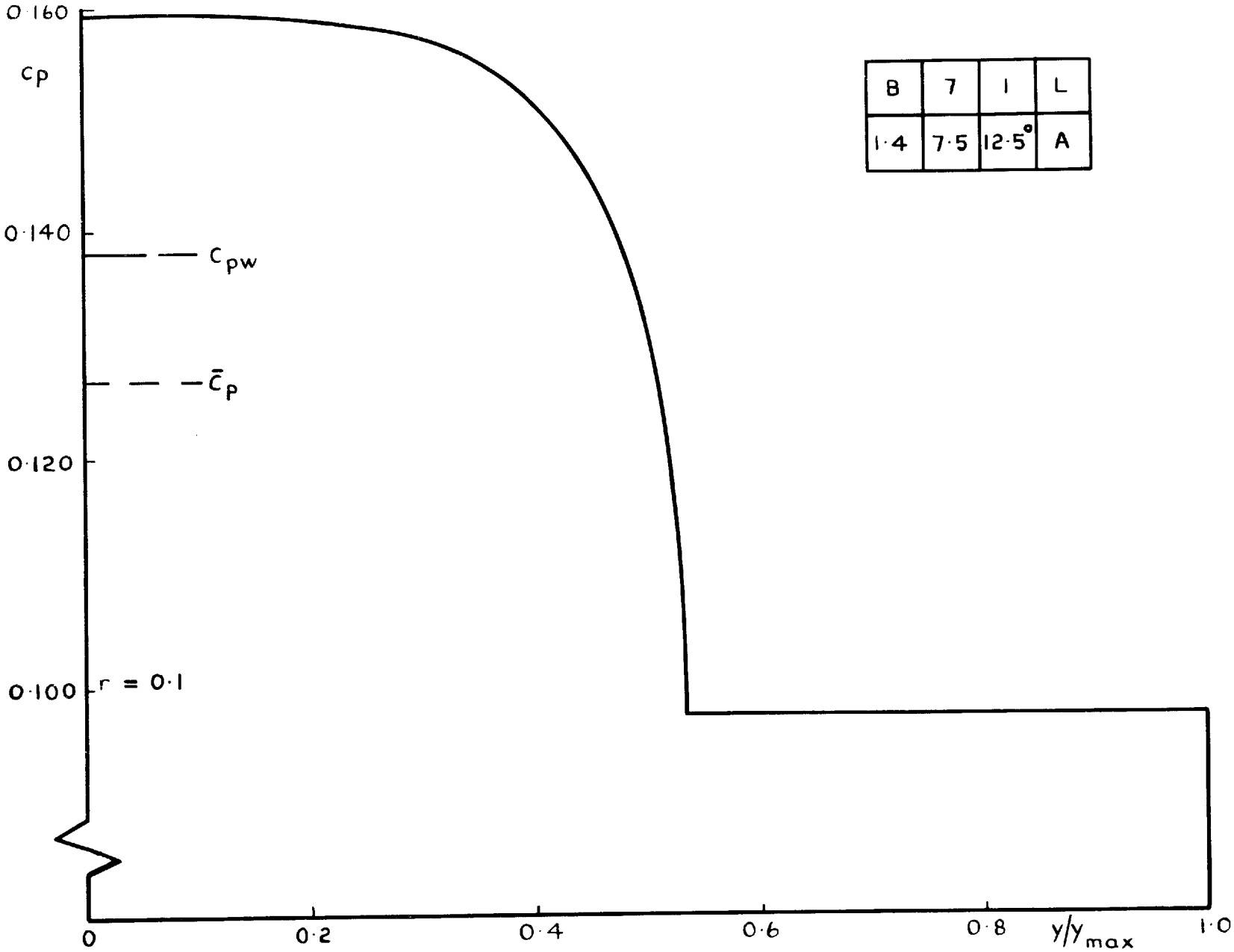

Fig. 24 Wing B: Pressure distribution lower surface $M = 7{\cdot}5$, $\gamma = 1{\cdot}4$, $\alpha = 12{\cdot}5^{\circ}$

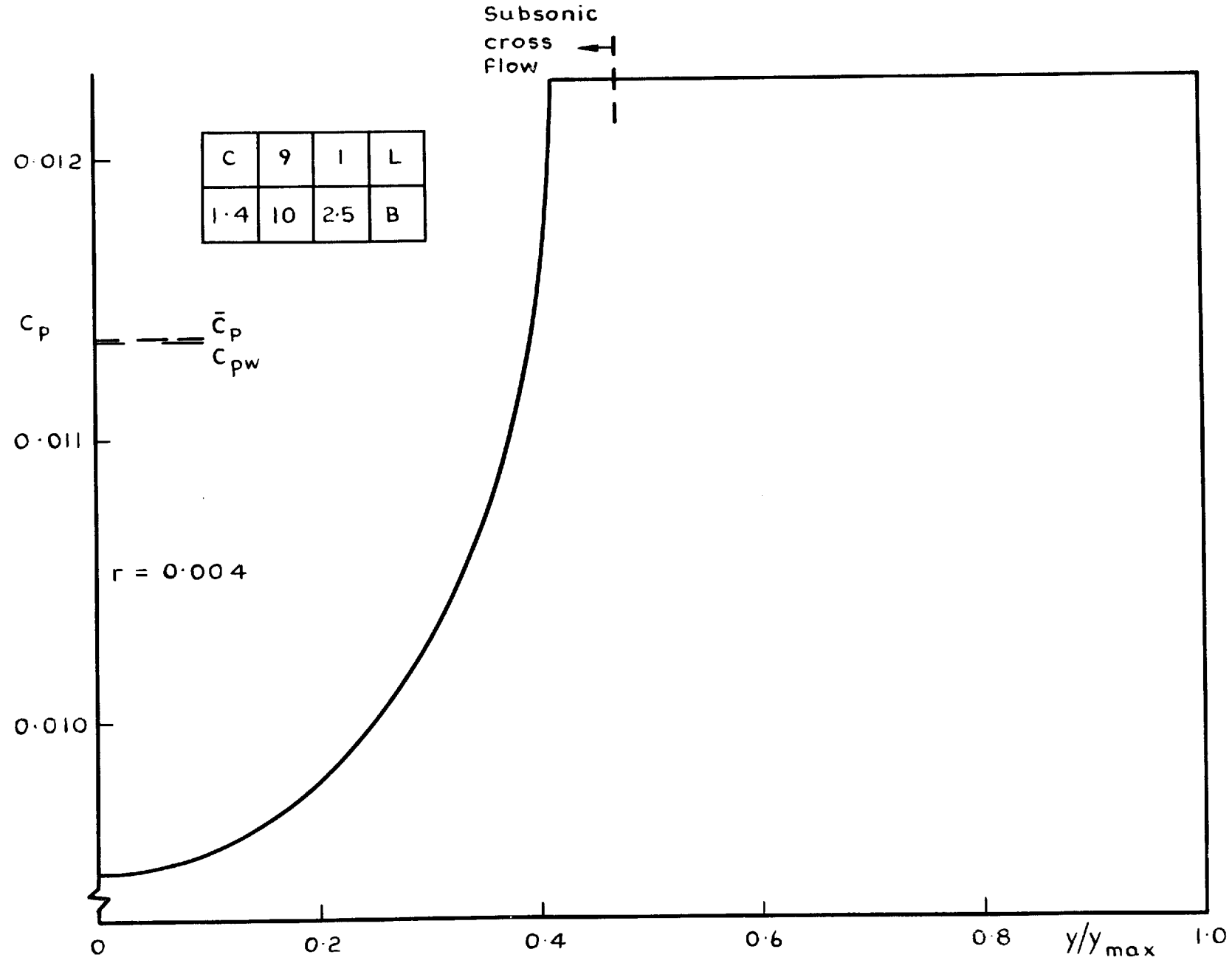

Fig. 25 Wing C: Pressure distribution lower surface M = 10, γ = 1·4, α = 2·5°

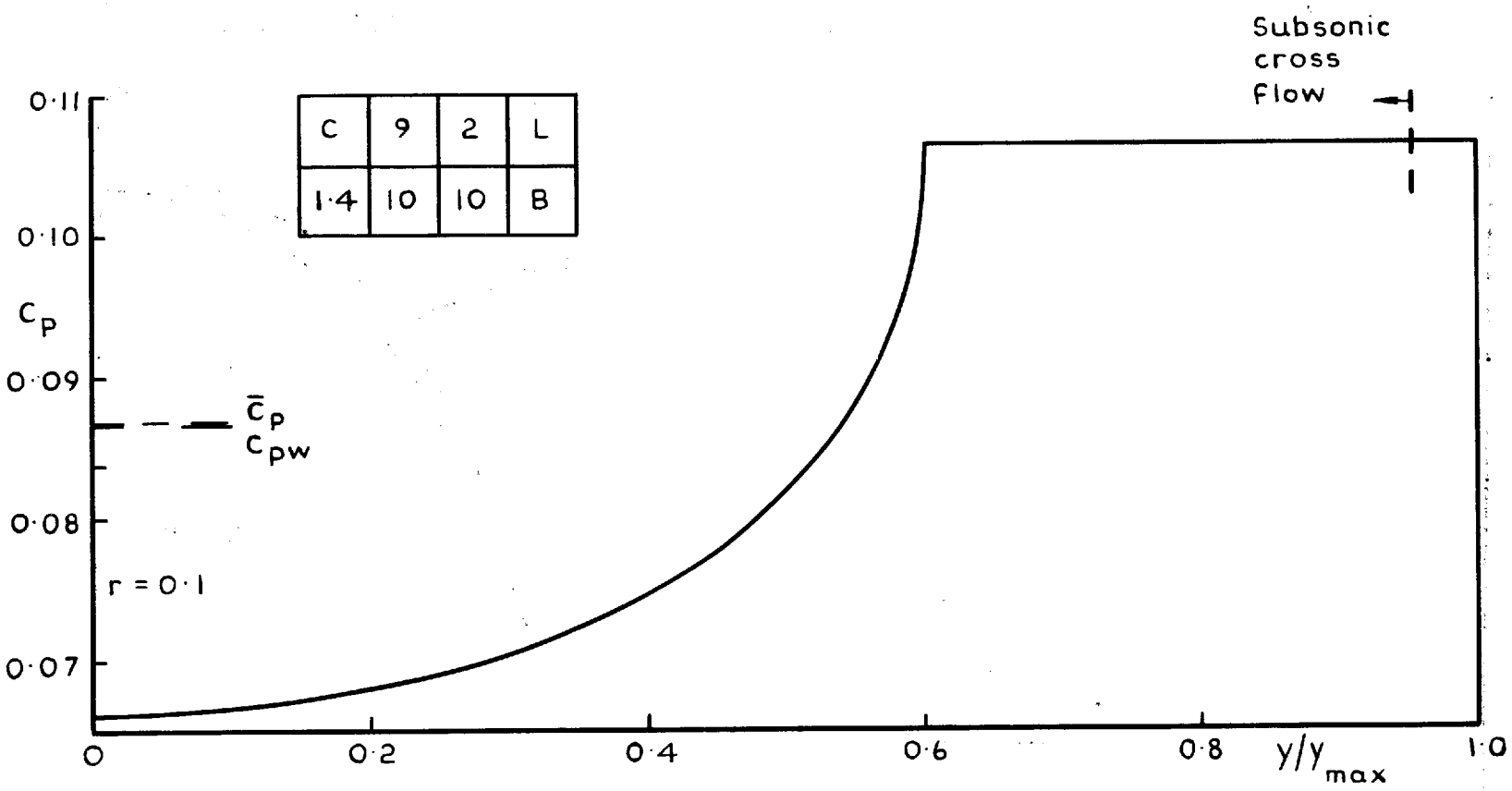

Fig. 26 Wing C: Pressure distribution lower surface $M = 10, \gamma = 1{\cdot}4, \alpha = 10^{\circ}$,

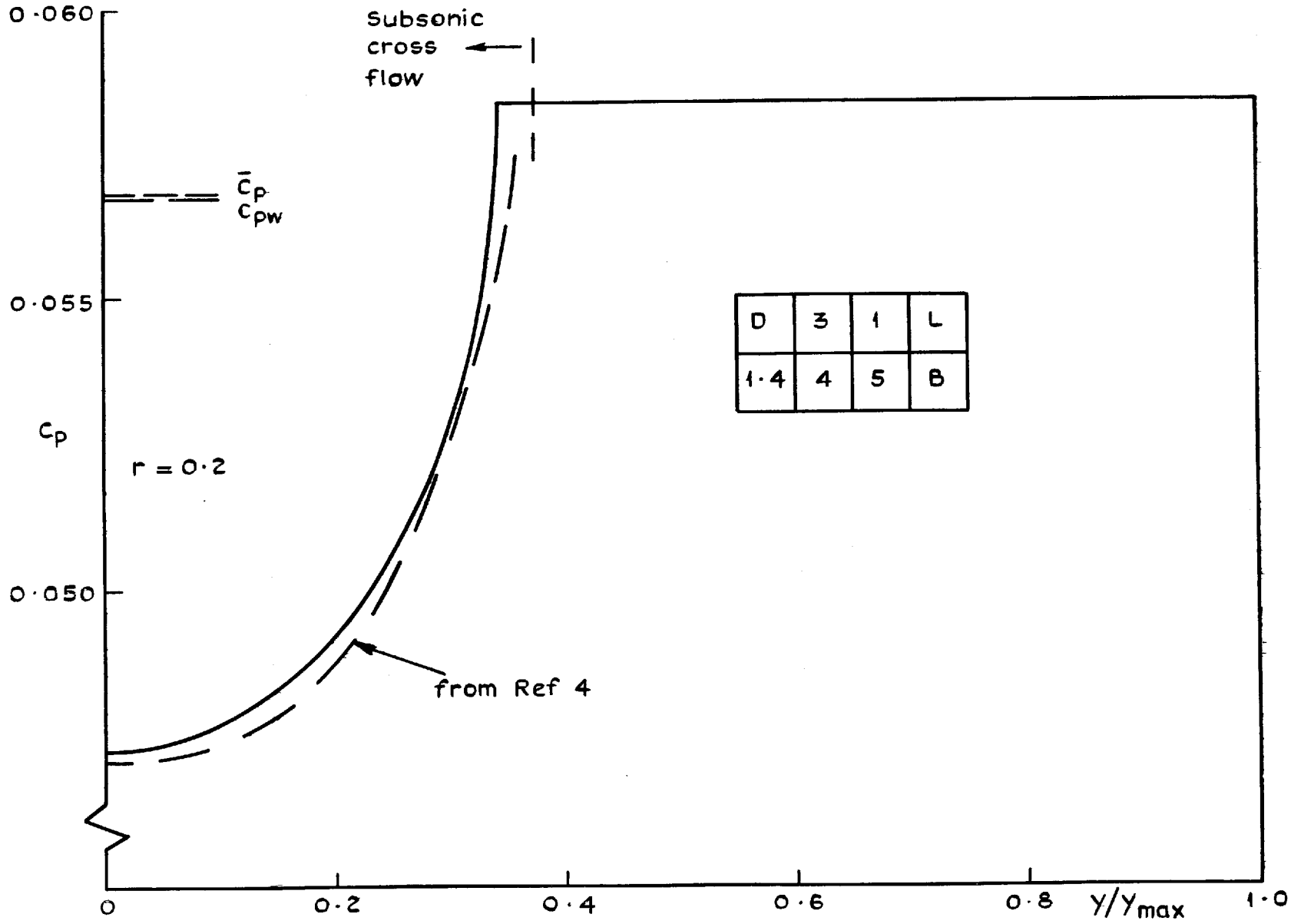

Fig.27 Wing D : Pressure distribution lower surface $M = 4$, $\gamma = 1{\cdot}4$, $\alpha = 5^\circ$

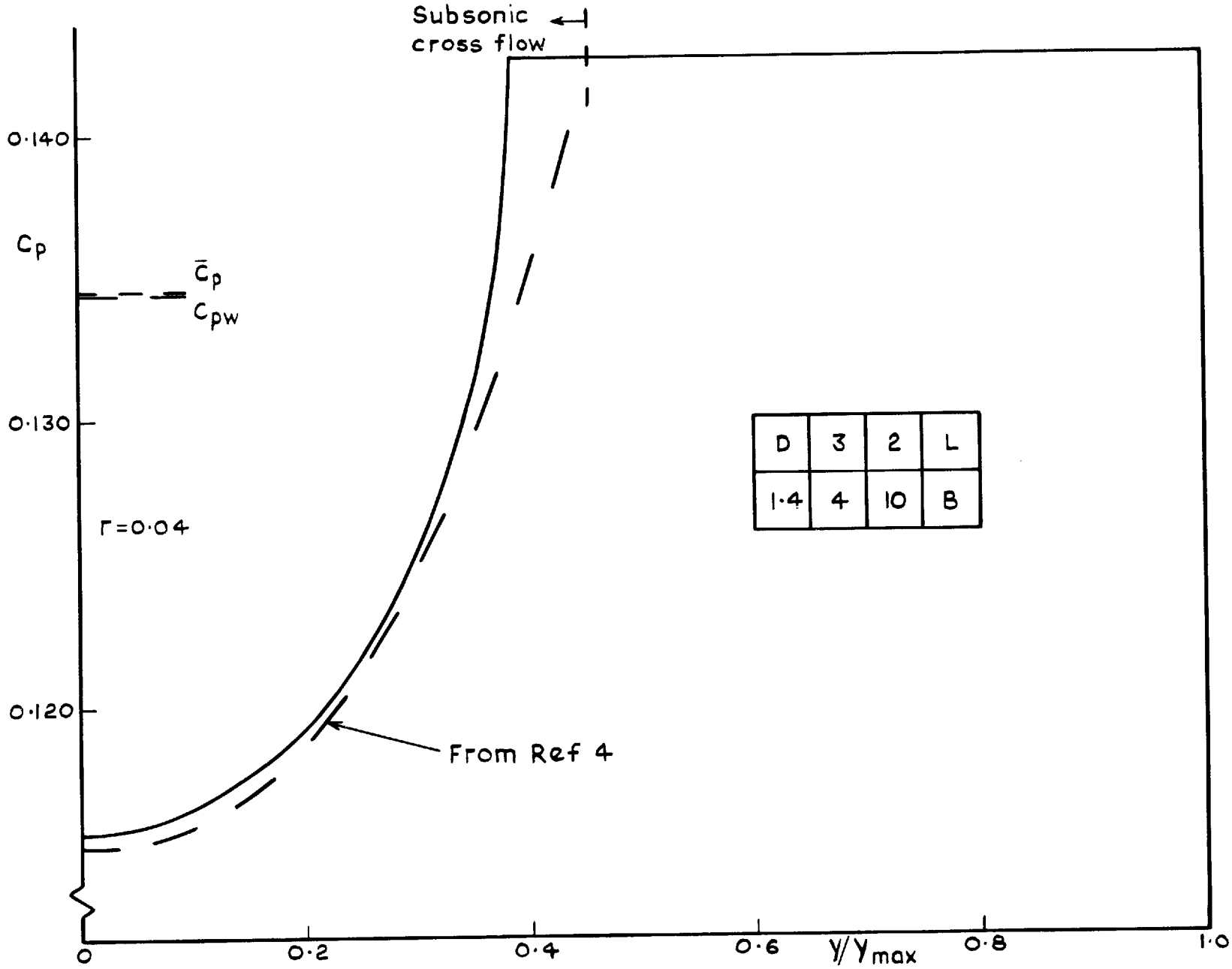

Fig. 28 Wing D: Pressure distribution lower surface $M = 4$, $\gamma = 1{\cdot}4$, $\alpha = 10^\circ$

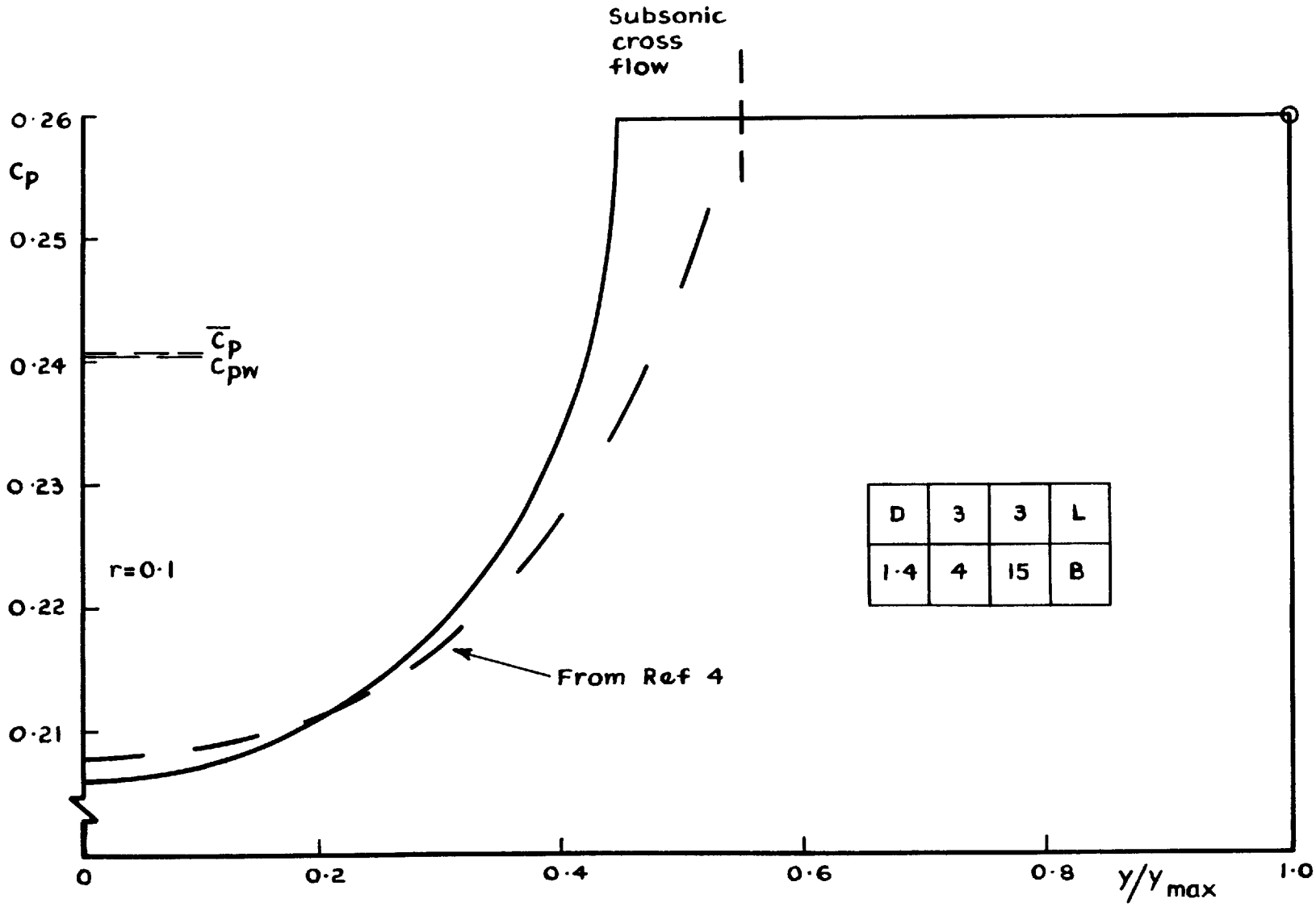

Fig.29 Wing D: Pressure distribution lower surface M=4, γ=1·4, α=15°

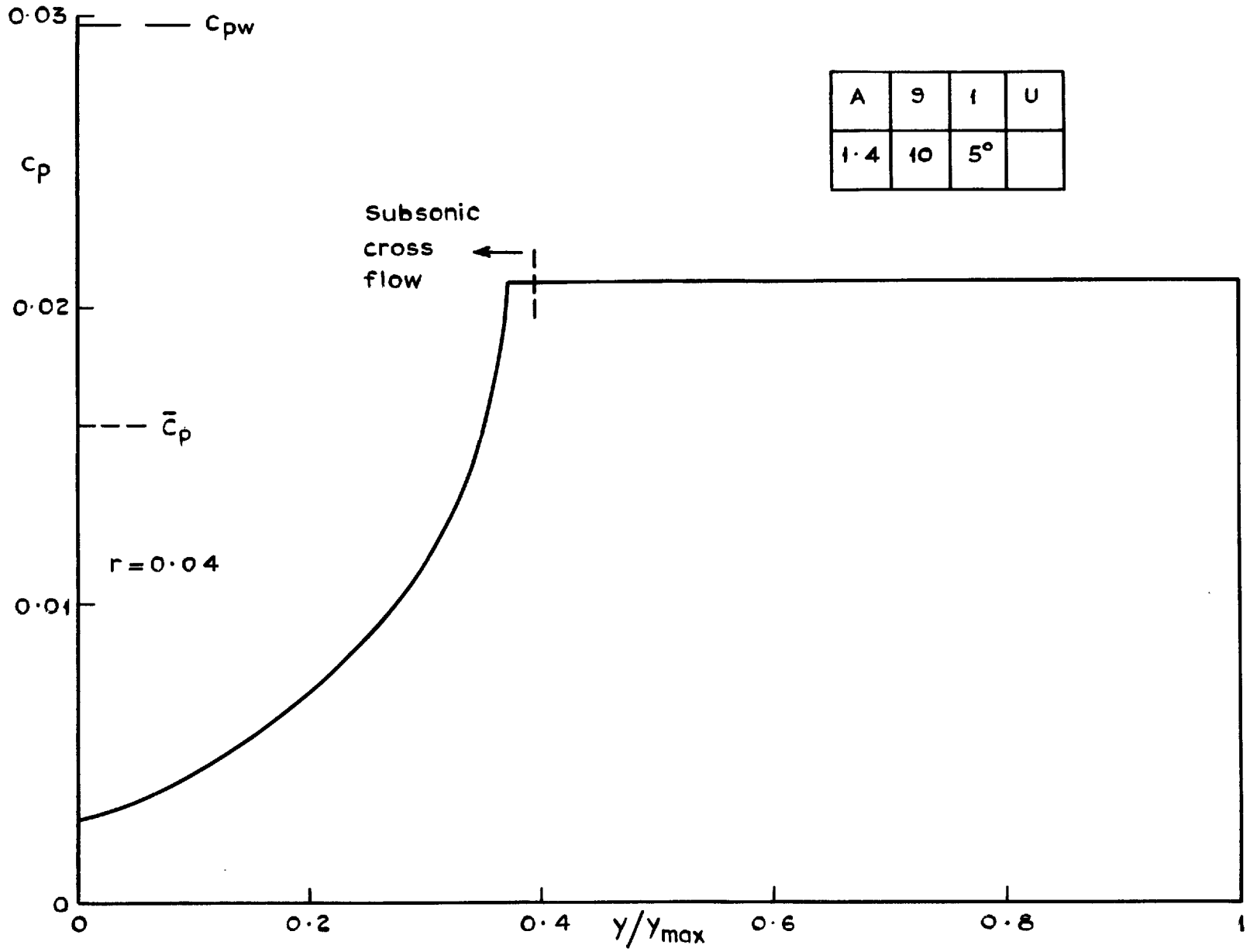

Fig.30 Wing A : Pressure distribution upper surface $M = 10, \gamma = 1 \cdot 4, \alpha = +5^{\circ}$

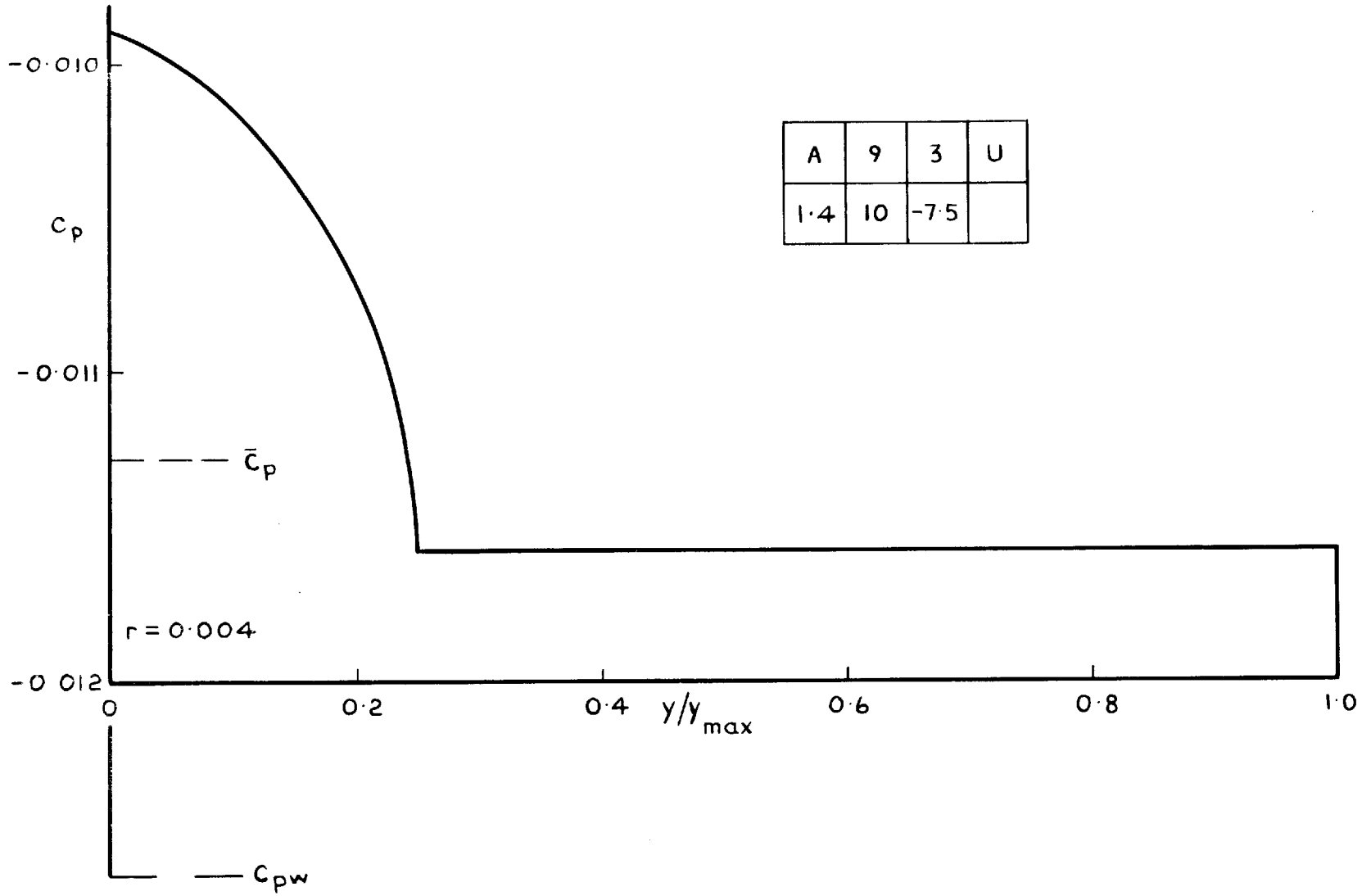

Fig. 31 Wing A: Pressure distribution upper surface $M = 10$, $\gamma = 1{\cdot}4$, $\alpha = -7{\cdot}5^{\circ}$

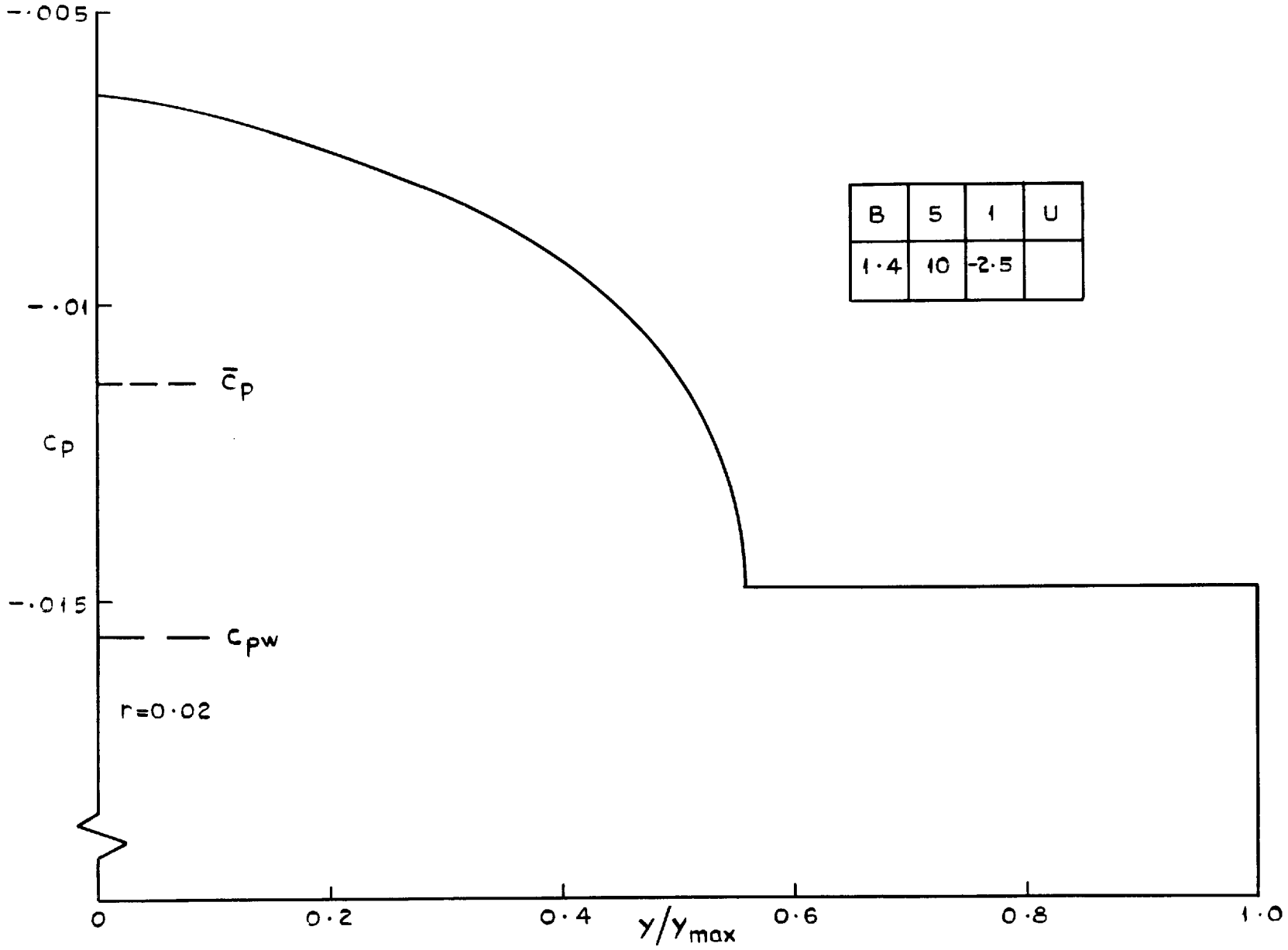

Fig. 32 Wing B : Pressure distribution upper surface $M = 5$, $\gamma = 1 \cdot 4$, $\alpha = -2 \cdot 5^{\circ}$

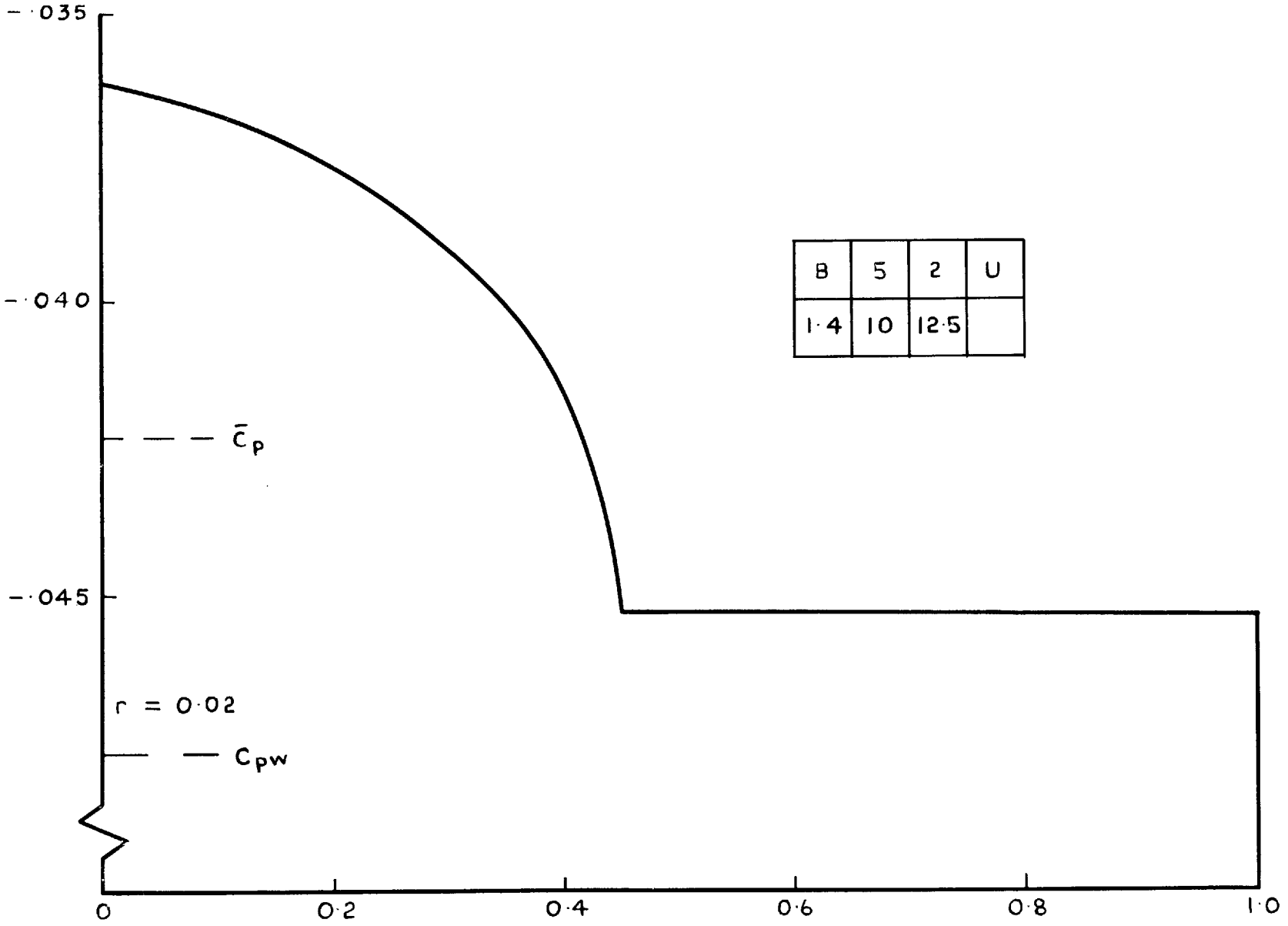

Fig. 33 Wing B: Pressure distribution upper surface $M = 5$, $\gamma = 1{\cdot}4$, $\alpha = 12{\cdot}5^\circ$

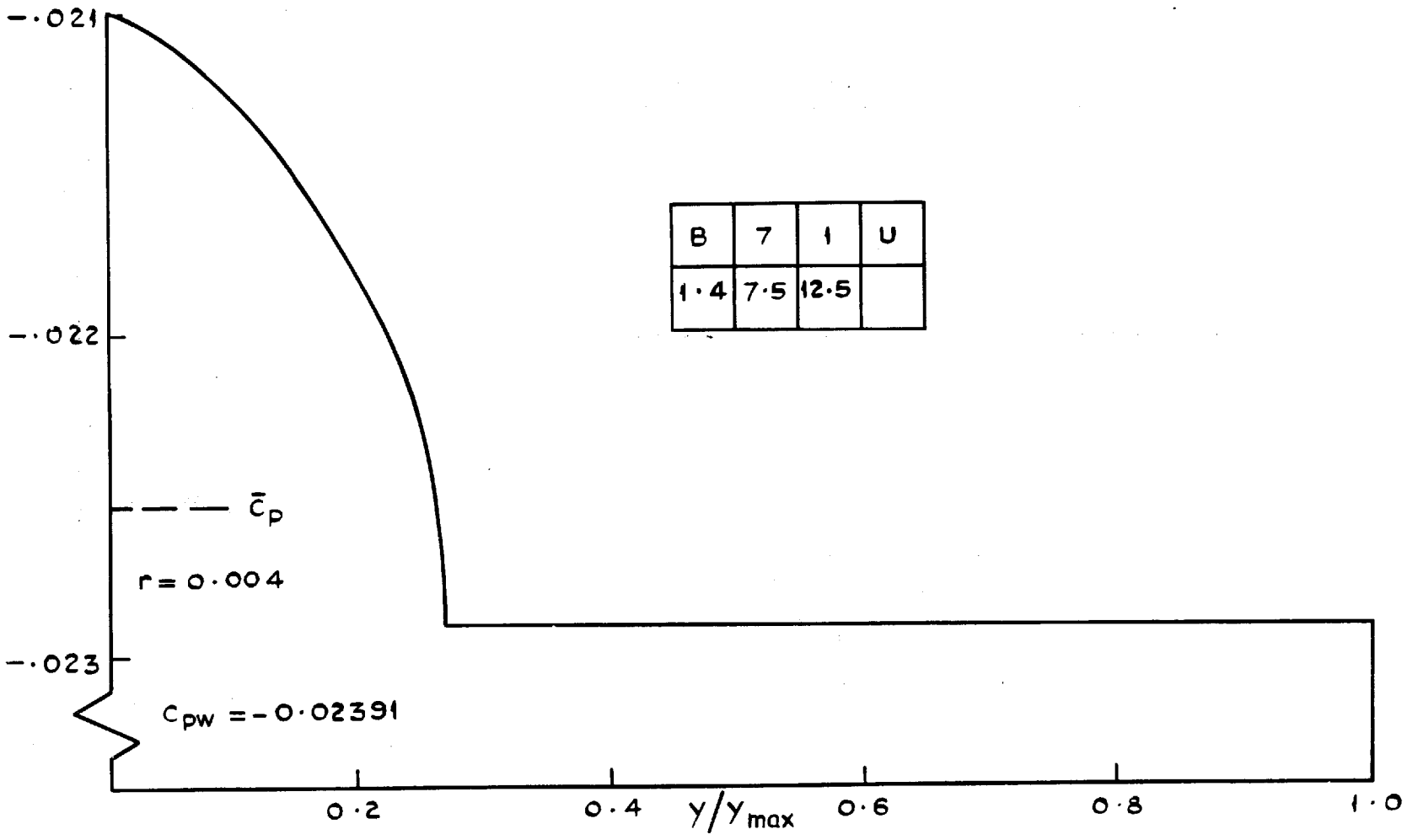

Fig.34 Wing B : Pressure distribution upper surface $M = 7{\cdot}5$, $\gamma = 1{\cdot}4$, $\alpha = 12{\cdot}5^{\circ}$

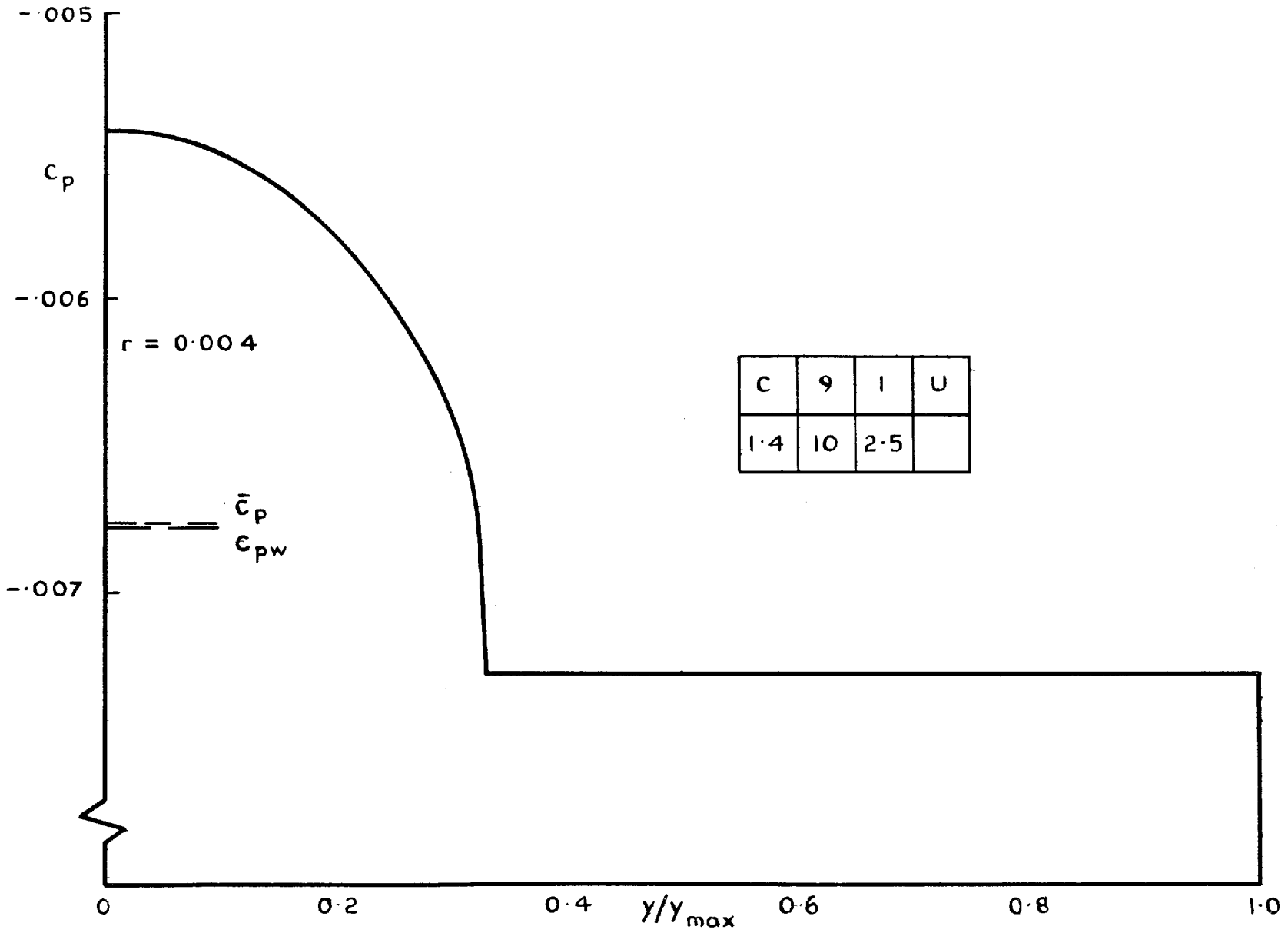

Fig. 35 Wing C: Pressure distribution upper surface M = 10, γ = 1·4, α = 2·5°

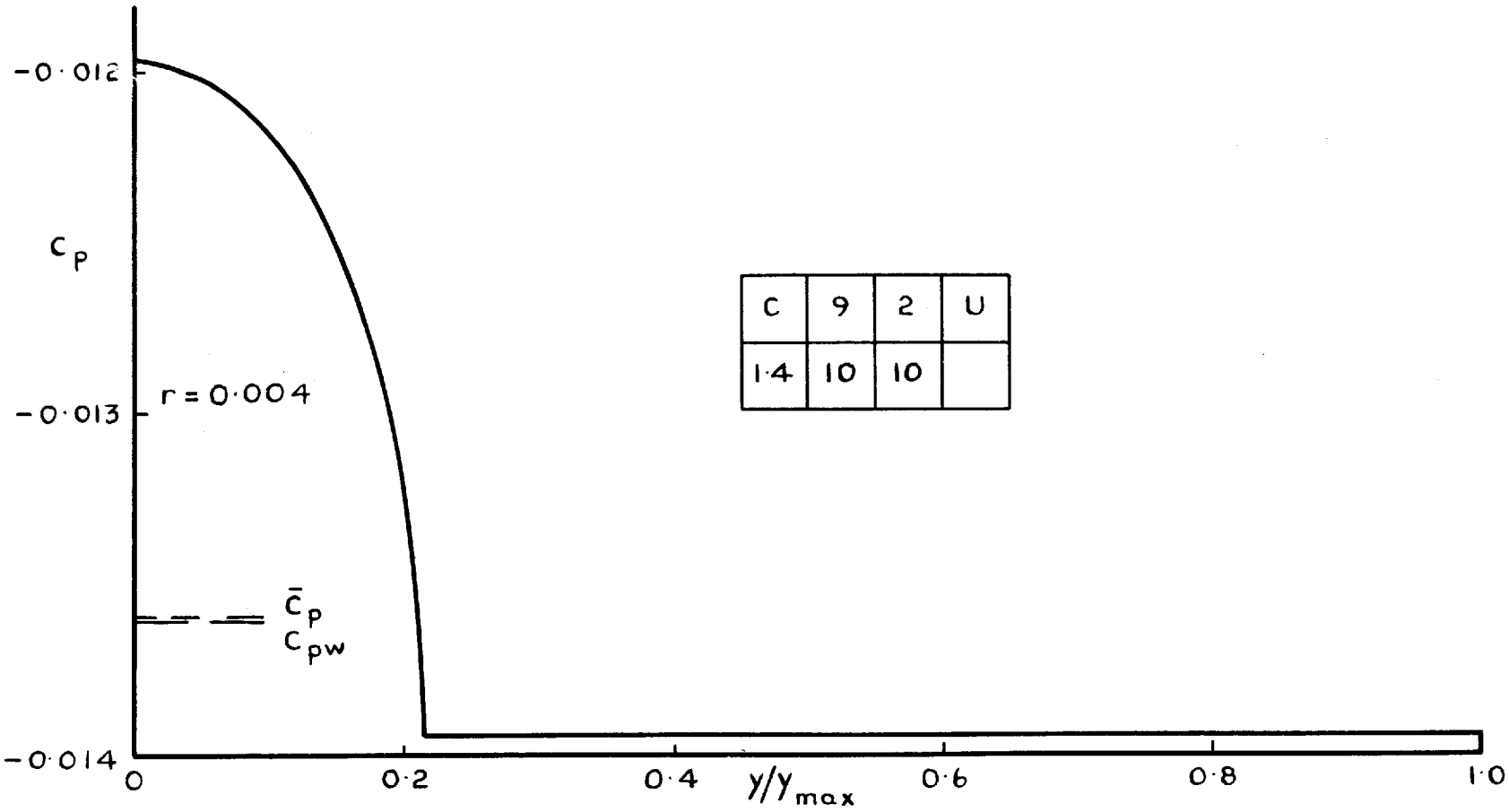

Fig. 36 Wing C: Pressure distribution upper surface $M = 10$, $\gamma = 1{\cdot}4$, $\alpha = 10^{\circ}$,

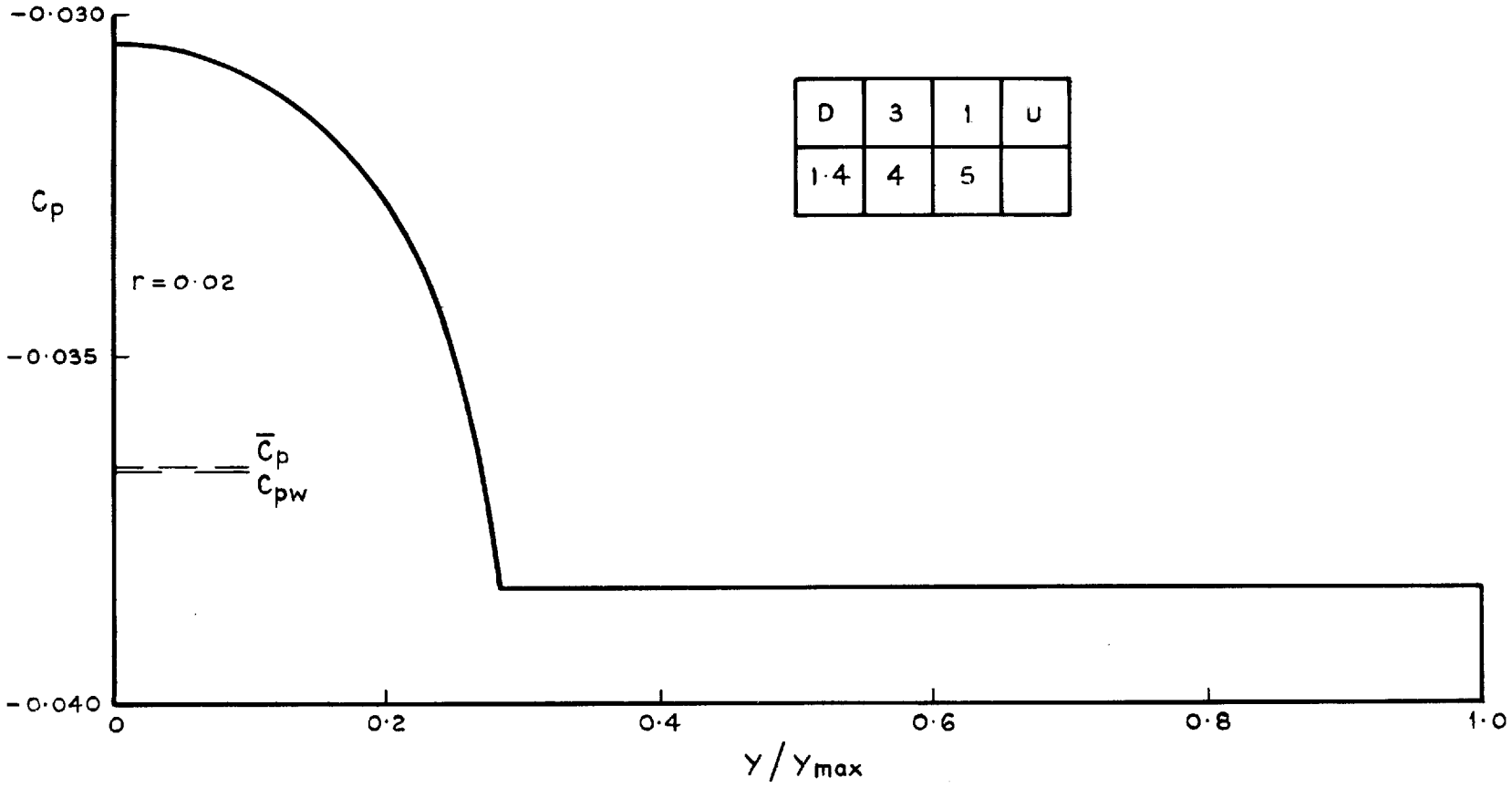

Fig. 37 Wing D: Pressure distribution upper surface $M = 4$, $\gamma = 1{\cdot}4$, $\alpha = 5^{\circ}$

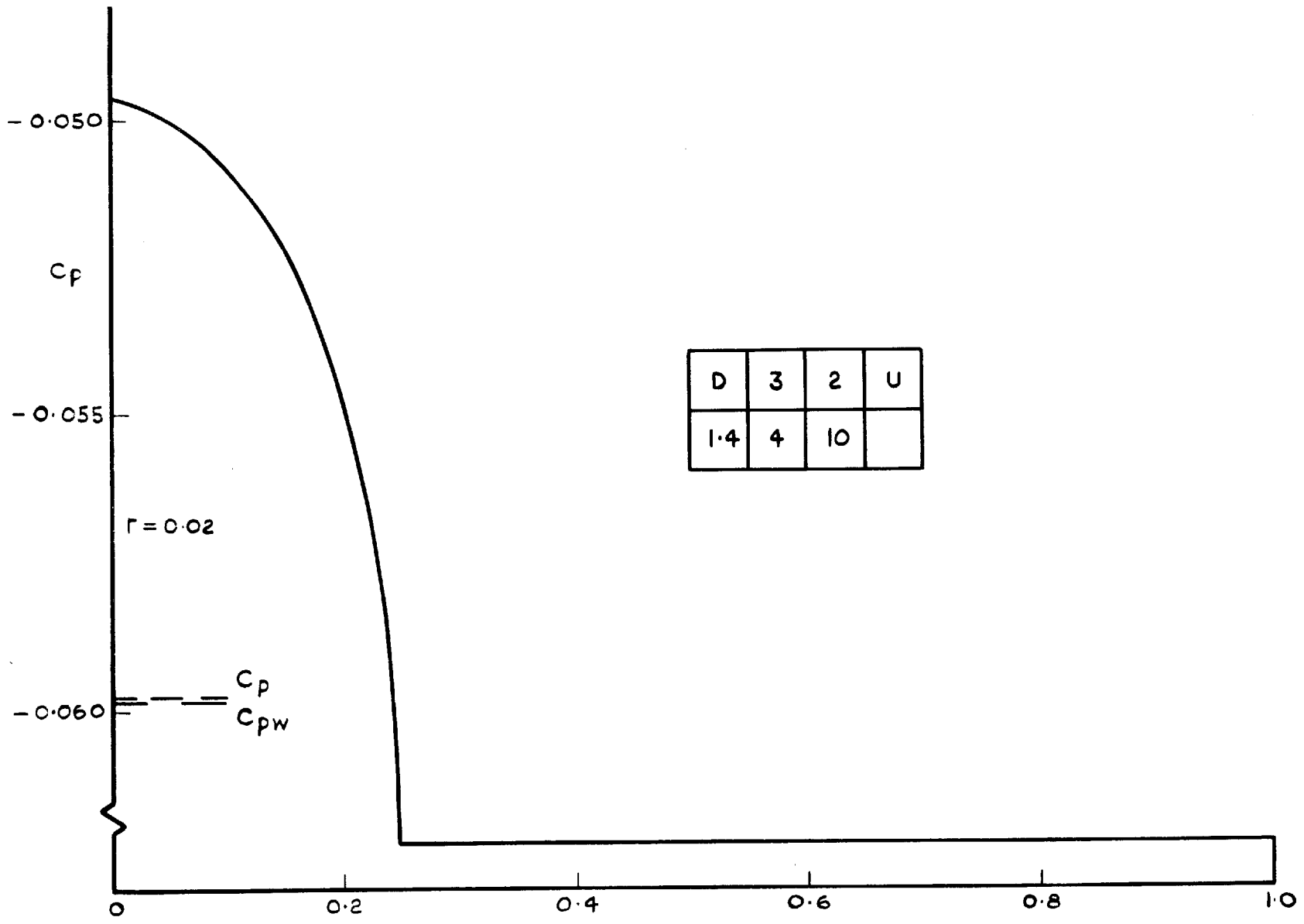

Fig. 38 Wing D: Pressure distribution upper surface $M = 4$, $\gamma = 1{\cdot}4$, $\alpha = 10^{\circ}$

Printed in England for Her Majesty's Stationery Office by the Royal Aircraft Establishment, Farnborough. Dd.502109. K.4.

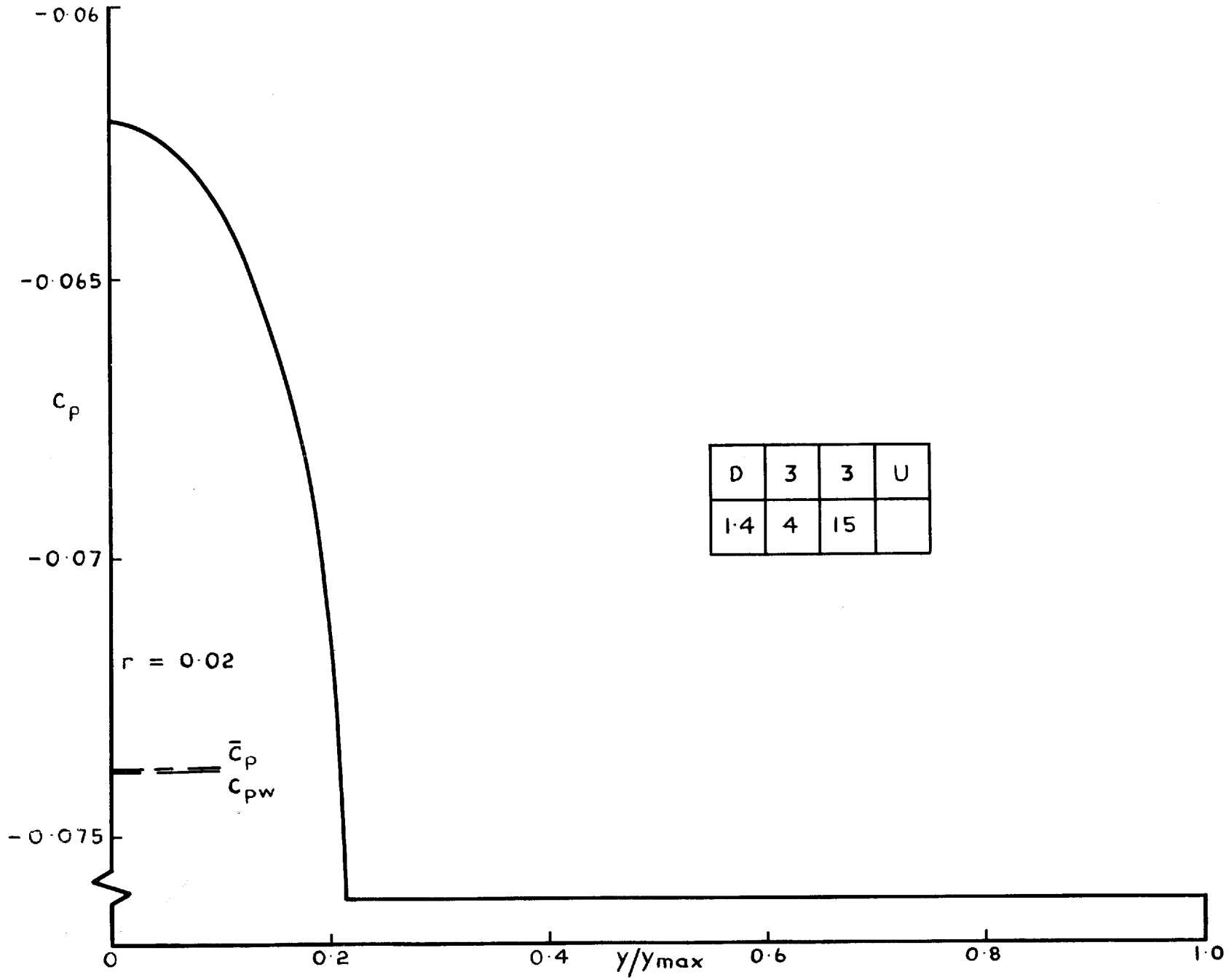

Fig. 39 Wing D: Pressure distribution upper surface $M = 4$, $\gamma = 1{\cdot}4$, $\alpha = 15^\circ$